Basic Physical Models

5.1 — Basic equations

As mentioned in chapter 1, writing the Navier-Stokes equations in terms of a derivative following the motion

$$\frac{D}{Dt} = \frac{\partial}{\partial t} + \mathbf{u} \cdot \nabla$$

provides a useful shorthand in Cartesian coordinates, but fails to account for all the nonlinear terms in the expressions for accelerations. The proper equations for various coordinate systems (or for general orthogonal cases) can be found in fluid dynamics textbooks such as (xx, xx, xx). We prefer a vector-invariant form

$$\frac{\partial}{\partial t}\mathbf{u} + (2\vec{\Omega} + \boldsymbol{\zeta}) \times \mathbf{u} = -\frac{1}{\rho}\nabla p - \nabla\frac{1}{2}|\mathbf{u}|^2 - \nabla\Phi + \mathit{Visc.} \tag{5.1}$$

where $\boldsymbol{\zeta}$ is the vorticity – the curl of the velocity

$$\boldsymbol{\zeta} = \nabla \times \mathbf{u} \tag{5.2}$$

(The common notation above for the curl indeed reduces to taking the cross-product of something that looks like a vector ∇ with $\mathbf{u}$ in Cartesian coordinates, but has a different form of the operator otherwise. I.e., the "∇" generally represents different operators in the gradient, divergence and curl. The notation does have the advantage of reminding us that the curl of a gradient and the divergence of a curl is zero. The forms in the coordinates we use are given in appendix 5.A.)

The physical interpretation of (5.1) is straightforward, given that the vorticity represents the local spin of the fluid: accelarations are associated with Coriolis forces arising from the local and planetary rotation, from gradients of the pressure and the Bernouilli term, from friction, and from gravity ($-\nabla\Phi = -g\hat{\mathbf{z}}$ where Φ includes both the gravitational and centrifugal potentials). For uniform density or under the Boussinesq approximation, the pressure and squared velcoity terms combine to give a Bernouilli potential $p/\rho + \frac{1}{2}|u|^2$, and the fluid will attempt to accelerate down the gradient of this function.

The viscous terms can be complicated, including variations with temperature (which can cause variations by a factor of xx [CRC Handbook], non-Newtonian effects, and a bulk viscosity from friction acting during compression (c.f. xx). For most problems, we ignore these subtleties since the "viscosity" represents turbulent mixing rather than molecular processes in any case and simply take

$$\mathit{Fric} = -\nu\nabla \times \boldsymbol{\zeta}$$

The mass

$$\frac{\partial}{\partial t}\rho + \nabla \cdot (\rho\mathbf{u}) = 0 \tag{5.3}$$

and salt

$$\frac{D}{Dt}S = \mathit{SaltDiffusion} \tag{5.4}$$

equations have been discussed in Ch. 1.

5.1.1 — Vorticity and potential vorticity

As discussed in Chapter 1, the vorticity $\boldsymbol{\zeta}$ plays a central role in large-scale dynamics. We can look at the way in which vorticity is generated by taking the curl of the momentum equation

$$\frac{\partial}{\partial t}\boldsymbol{\zeta} + \nabla \times [(2\vec{\Omega} + \boldsymbol{\zeta}) \times \mathbf{u}] = \frac{1}{\rho^2}\nabla\rho \times \nabla p + \nabla \times \mathit{Visc} \tag{5.5}$$

In cartesian form, this can be written

$$(\frac{\partial}{\partial t} + \mathbf{u} \cdot \nabla)(\boldsymbol{\zeta} + 2\vec{\Omega}) + (\boldsymbol{\zeta} + 2\vec{\Omega})\nabla \cdot \mathbf{u} - [(\boldsymbol{\zeta} + 2\vec{\Omega}) \cdot \nabla]\mathbf{u} = \frac{1}{\rho^2}\nabla\rho \times \nabla p + \nu\nabla^2\boldsymbol{\zeta} \tag{5.6}$$

Thus the gradients of density along pressure surfaces (which are close to level in the sense of constant geopotential) can produce vorticity and motion. Indeed, geostrophic calculations are carried out using the specific volume anomaly $[\alpha(S,T,p) - \alpha(35,0,p)$ with $\alpha = 1/\rho]$ to remove the large but unimportant variation with pressure.

Frictional forces with walls can produce vorticity and diffuse it into the interior. For example, uniform flow in the x direction impinging on a flat plate will develop shear $\frac{\partial}{\partial z}u > 0$ above the plate as the velocity in brought to zero on the plate. This shear corresponds to $\zeta_2 > 0$ near the plate. Thus irrotational flow is generally not obtainable, although the concept remains a useful abstraction for surface waves and small-scale, low Reynolds number flows.

In addition to the generation terms on the r.h.s. of 5.xx, the vortex stretching and tilting terms $[(\boldsymbol{\zeta} + 2\vec{\Omega}) \cdot \nabla]\mathbf{u}$ dramatically alter the vorticity distribution. To understand these terms, let us consider the vertical component

$$\frac{D}{Dt}(\zeta_3 + f) = (\boldsymbol{\zeta}_h + 2\vec{\Omega}_h) \cdot \nabla_h w + (\zeta_3 + f)\frac{\partial w}{\partial z}$$

(assuming the velocity is nondivergent, $\hat{\mathbf{z}} \cdot \nabla\rho \times \nabla p = 0$, and ignoring friction). The h subscript refers to the horizontal components; i.e., $\boldsymbol{\zeta}_h = (\zeta_1, \zeta_2, 0)$. The first two terms generate vertical vorticity by rotating a horizontal vector around the perpendicular axis: $\frac{\partial w}{\partial x} > 0$ corresponds to rotation in the counterclockwise sense around the y-axis, which will turn a vorticity vector in the x-direction into a more vertical vector. These are "tilting" terms. The $(\zeta_3 + f)\frac{\partial w}{\partial z}$ represents "stretching" which elongates a vortex tube. By mass/volume conservation, the horizontal area of the tube will shrink; conservation of circulation implies the product of vorticity and area is constant so that the vorticity must grow. Often we think of this in terms of the ice-skater effect – decreasing the moment of inertia leads to more rapid spinning. The fluid system is a bit more complicated, as we shall see when we derive the full potential vorticity conservation law, but this analogy gives us a feel for the way the tradeoffs work.

Potential vorticity

Since the vorticity is a vector quantity, complexities arise when working in non-cartesian geometries. Instead, meteorologists and oceanographers since Ertel (19xx) have encapsulated many of the important elements of vorticity dynamics in a scalar quantity, the potential vorticity

$$q = \frac{1}{\rho}(\boldsymbol{\zeta} + 2\vec{\Omega}) \cdot \nabla\chi$$

The PV will be conserved under inviscid dynamics if

$$\frac{D}{Dt}\chi = 0 \quad \text{and} \quad \nabla\chi \cdot (\nabla\rho \times \nabla p) = 0$$

(see appendix 5.A). In the Boussinesq case, the bouyancy B satisfies these conditions since $\rho = \rho_0(1 - B/g)$, and density is conserved. We can now interpret Ertel's theorem: $|\nabla B|$ is inversely proportional to the thickness between isopycnals, and conservation of mass implies that $\rho\Delta z A \propto \rho A/|\nabla B|$ for a small cylinder of fluid with area A on a constant B surface. The net circulation around the cylinder is $A(\boldsymbol{\zeta} + 2\vec{\Omega}) \cdot \nabla B/|\nabla B|$. This is also conserved by Kelvin's/ Bjerknes' theorem – since $\rho =$ const., the net pressure force around the circuit $\oint \frac{1}{\rho}\nabla p = \frac{1}{\rho}\oint \nabla p$ is zero as is the net graviational force. Thus the circulation will not increase. Eliminating A between these two conserved properties shows that q is also constant following the motion. If ∇B decreases, the fluid will be stretched normal to the B surfaces, and the vorticity in that direction will increase.

5.1.2 — Thermodynamics

Previously, we introduced the Boussinesq approximation and effectively bypassed the thermodynamic equation. However, not only is familiarity with the concepts of potential temperature and potential density important, but also GCM's do need to deal with some more correct representation of the relationship between temperature, salinity, pressure, and density. The conventional approach (e.g., Fofonoff, 19xx) starts with an equation of state in terms of the measurable properties (p, T, S)

$$\rho = \rho(S, T, p) \tag{5.7}$$

and the first two laws of thermodynamics which imply that

$$d\varepsilon = Td\eta - pd\alpha + \mu dS \quad , \quad Td\eta = \mathcal{H}$$

where ε and η are the internal energy and entropy per unit mass, μ is the chemical potential, $\alpha = 1/\rho$ is the specific volume, and $\mathcal{H}$ is the heating rate.† Feistel (2005) offers an elegant

† Built in is the assumption that the various elements making up sea salt appear in the same relative proportions; "salinity" then measures the total amount of dissolved sustance per unit seawater mass. The chemical potential is then a weighted average of the ones for individual elements expressing how the internal energy changes as the foreign element is added to water.

alternative: the Gibbs function $G = \varepsilon - T\eta + p\alpha$, expresses the thermodynamics directly in terms of the measurables:

$$dG = -\eta dT + \alpha dp + \mu dS \quad ;$$

given an expression for $G(S, T, p)$, we can find the specific volume, entropy, and chemical potential

$$\alpha = \frac{\partial G}{\partial p} \quad , \quad \eta = -\frac{\partial G}{\partial T} \quad . \quad \mu = \frac{\partial G}{\partial S}$$

The entropy of the fluid changes by heating, which we can also express as the divergence of the heat flux vector $\mathbf{Q}$:

$$T\frac{D}{Dt}\eta = T\frac{\partial \eta}{\partial T}\frac{D}{Dt}T + T\frac{\partial \eta}{\partial S}\frac{D}{Dt}S + T\frac{\partial \eta}{\partial p}\frac{D}{Dt}p = \mathcal{H} = -\nabla \cdot \mathbf{Q}$$

The specific heat at constant pressure, c_p, is defined by $T\frac{\partial}{\partial T}\eta$; it and the other terms can be found by differentiating the Gibbs relations above. We arrive at

$$c_p\frac{D}{Dt}T - T\frac{\partial \mu}{\partial T}\frac{D}{Dt}S - T\frac{\partial \alpha}{\partial T}\frac{D}{Dt}p = \mathcal{H} = -\nabla \cdot \mathbf{Q} \tag{5.8}$$

In principle, equations 5.1-6 provide a predictive system allowing us to step the dynamics forward in time; however, one of the parts is implicit in that the changes in α must be consistent with the changes in p and T together with the equation of state. To avoid this problem, we can use the entropy equation to predict the changes in density:

$$\begin{aligned}\frac{D}{Dt}\rho &= \frac{\partial \rho}{\partial T}\frac{D}{Dt}T + \frac{\partial \rho}{\partial S}\frac{D}{Dt}S + \frac{\partial \rho}{\partial p}\frac{D}{Dt}p \\ &= \left[\frac{\partial \rho}{\partial p} - \frac{T}{c_p}\left(\frac{1}{\rho}\frac{\partial \rho}{\partial T}\right)^2\right]\frac{D}{Dt}p + \left[\frac{\partial \rho}{\partial S} + \frac{T}{c_p}\frac{\partial \rho}{\partial T}\frac{\partial \mu}{\partial T}\right]\frac{D}{Dt}S - \frac{1}{c_p}\frac{\partial \rho}{\partial T}\nabla \cdot \mathbf{Q}\end{aligned}$$

The first term on the right hand side is related to the sound speed (as we shall see).

$$\frac{D}{Dt}\rho = c_s^{-2}\frac{D}{Dt}p + \left[\frac{\partial \rho}{\partial S} + \frac{T}{c_p}\frac{\partial \rho}{\partial T}\frac{\partial \mu}{\partial T}\right] SaltDiffusion - \frac{1}{c_p}\frac{\partial \rho}{\partial T}\nabla \cdot \mathbf{Q} \tag{5.9}$$

The second term in the coefficient for salinity is a few percent of $\frac{\partial \rho}{\partial S}$ and is generally ignored. If we regard the speed of sound and the coefficients of the salt diffusion and the heating as functions of ρ, p and S, rather than of temperature, the equations 5.1-5,7 can be advanced directly: given $\mathbf{u}$, ρ, S, and p, we can find the increment in $\mathbf{u}$ from 5.1, in ρ from 5.3, in S from 5.4, and in p from 5.3 & 5.6. Such an approach runs into Richardson's (19xx) problem; the high-speed sound waves induced by small imbalances in the mass fluxes will quickly swamp the interesting signals. We shall discuss filtering approximations that eliminate this problem later.

Potential Temperature and Density

Sea water is not incompressible (ρ varies by several percent from the surface to depth; almost all of this results from the 500 atmospheres of pressure at the ocean bottom). The dynamically significant variability from the viewpoint of the momentum equations is the vorticity generating part, found by taking the curl of the momentum equation

$$\frac{\partial}{\partial t}\boldsymbol{\zeta} + \nabla \times [(2\vec{\Omega} + \boldsymbol{\zeta}) \times \mathbf{u}] = \frac{1}{\rho^2}\nabla\rho \times \nabla p + \nabla \times \mathit{Visc}$$

In cartesian form, this can be written

$$(\frac{\partial}{\partial t} + \mathbf{u}\cdot\nabla)(\boldsymbol{\zeta} + 2\vec{\Omega}) + (\boldsymbol{\zeta} + 2\vec{\Omega})\nabla\cdot\mathbf{u} - [(\boldsymbol{\zeta} + 2\vec{\Omega})\cdot\nabla]\mathbf{u} = \frac{1}{\rho^2}\nabla\rho\times\nabla p + \nu\nabla^2\boldsymbol{\zeta}$$

Thus the gradients of density along pressure surfaces (which are close to level in the sense of constant geopotential) can produce vorticity and motion. Indeed, geostrophic calculations are carried out using the specific volume anomaly $[\alpha(S,T,p) - \alpha(35,0,p)]$ to remove the large but unimportant variation with pressure.

But we also want to isolate the pressure-induced compression in the thermodynamic equation, by distinguishing *adiabatic* motions for which entropy is conserved versus *diabatic motions* wherein the entropy changes because of heating or salt diffusion. Using "potential temperature," defined as the temperature a parcel of fluid would have if the pressure is adjusted without exchange of heat or salt to a reference value p_r, allows us to remove the compressibility effects. We can think of the potential temperature θ as entropy written in T units: the implicit equation

$$\eta(S,\theta,p_r) = \eta(S,T,p) \tag{5.10}$$

can be solved iteratively (Feister, 2005) to give $\theta(S,T,p,p_r)$. We can plot the isentropes (figure 5.xx) by integrating

$$0 = \delta\eta = \frac{\partial\eta}{\partial T}\delta T + \frac{\partial\eta}{\partial p}\delta p \quad \Rightarrow \quad \frac{\delta T}{\delta p} = -\frac{\frac{\partial\eta}{\partial p}}{\frac{\partial\eta}{\partial T}} = \frac{T}{c_p}\frac{\partial\alpha}{\partial T}$$

If we start the isentrope at pressure p_r and temperature T_0, θ will be equal to T_0 all along the curve (figure 5.xx). Usually, the calculation is done in reverse: starting with T and p, we back up adiabatically to pressure p_r; the final temperature is the θ value of the water parcel. The adiabatic increase in temperature is order 0.1 degrees C per kilometer in depth or 10^{-4} $^{\circ}$C/*decibar*.

Figure 5.1: Potential temperature vs. pressure, temperature, and salinity.

We can define potential density similarly; however, the lines of constant entropy for different salinities will diverge in the ρ, p plane just as they do in the T, p plane. Therefore two parcels at some pressure other than the reference value can have the same potential density but different actual densities. So, rather than using potential density, we prefer writing the actual density as a function of θ, S, and p (we can do this by solving for T as in figure 5.xx or from 5.xx and substituting in the formula for the density; however, McDougall *et al.*19xx give direct expressions).

Differentiating 5.xx gives the dynamical equation for potential temperature (ignoring the heating arising from diffusion of salt)

$$\frac{\partial \eta}{\partial \theta} \frac{D}{Dt} \theta = -\frac{1}{T} \nabla \cdot \mathbf{Q}$$

or

$$\frac{D}{Dt} \theta = -\frac{\theta}{T c_p(\theta, S, p_r)} \nabla \cdot \mathbf{Q} \tag{5.11}$$

(where T will now be a function of θ, S, and p; see again figure 5.xx).

Simplified thermodynamics

For more idealized modelling, we can define a simplified thermodynamics by assuming the adiabatic compressibility

$$K_a = \frac{\partial}{\partial p} \ln \rho(\theta, S, p) = \rho^{-1} c_s^{-2}$$

is constant or a function only of pressure. For an ideal gas, $K_a = c_v/c_p p$, so this *ansatz* works exactly. For sea water, the variations in K_a are small to begin with (around 10%) and the temperature and salinity effects cause changes of 5% in the surface layers but only one or two percent in the deep ocean (figure 5,xx). When we make this assumption, we can define $\mathcal{K}_a$ as the integral with respect to p of K_a; adiabatically, then

$$\frac{D}{Dt} \ln \rho - K_a \frac{D}{Dt} p = 0 \quad \Rightarrow \quad \frac{D}{Dt} \ln \rho - \mathcal{K}_a(p) = 0$$

Thus we have a conserved entropy-like quantity defined in terms of density and pressure.

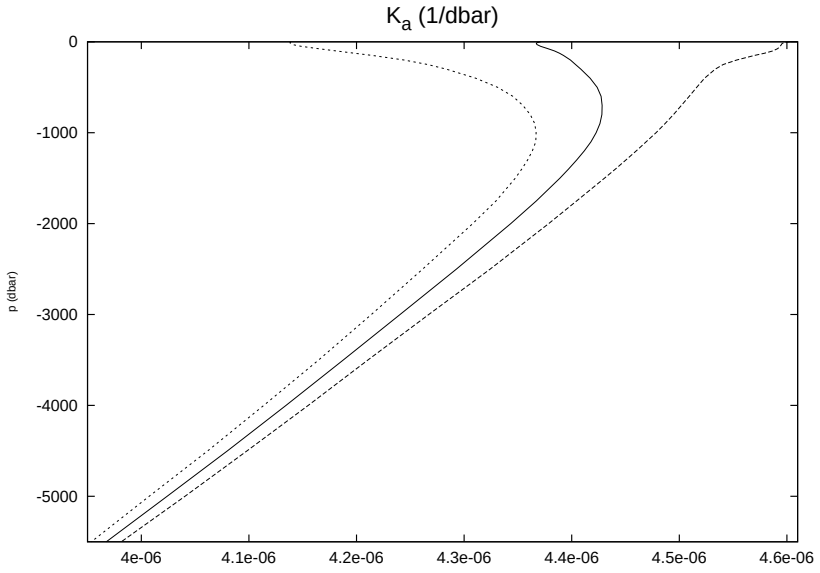

Figure 5.2: K_a from the World Ocean Atlas data, showing the means with one standard deviation at each depth level

5.1.3 — Hydrostatic state

By far the biggest contribution to the deep pressure is the weight of the water above; the fluctuating pressure gradients are much, much smaller than g. We can usefully divide the pressure and specific volume into hydrostatically balanced parts which depend only on depth and the deviations

$$p = \overline{p} + \rho\phi \quad , \quad \rho = \frac{\overline{\rho}}{1+\sigma} \quad \text{with} \quad \nabla\overline{p} = -\overline{\rho}\nabla\Phi$$

Then the forcing terms for the momentum become

$$-\frac{1}{\rho}\nabla p - \nabla\Phi = -\nabla\phi - \phi\frac{1}{\rho}\nabla\rho + \sigma\nabla\Phi \simeq -\nabla\phi - \phi\nabla\ln\overline{\rho} + \sigma\nabla\Phi$$

(since, as we shall see, $\sigma \sim 10^{-3}$). If we define a basic state version of the compressibility

$$\overline{K} = \frac{1}{\overline{\rho}}\frac{\delta\overline{\rho}}{\delta\overline{p}}$$

out pressure and gravitational forces become

$$-\nabla\phi + (\sigma + \overline{\rho}\overline{K}\phi)\nabla\Phi$$

We can use the rewritten density and pressure terms in the thermodynamic equation; however the case with the simplified thermodynamics is the most straightforward

$$\frac{D}{Dt}[-\ln\overline{\rho} + \mathcal{K}_a(\overline{p})] + \frac{D}{Dt}[\ln(1+\sigma) + \mathcal{K}_a(\overline{p}+\rho\phi) - \mathcal{K}_a(\overline{p})] = 0$$

so that to the relevant order

$$\frac{D}{Dt}[g\sigma + g\overline{\rho}\overline{K}_a\phi] + w\overline{N}^2 = \frac{D}{Dt}B + w\overline{N}^2 = 0$$

with $B = g\sigma + g\overline{\rho}\overline{K}_a\phi$ being the "potential buoyancy" and

$$\overline{N}^2 = g^2\overline{\rho}(\overline{K} - \overline{K}_a) = -g\frac{\partial}{\partial z}\ln\overline{\rho} - \frac{g^2}{\overline{c}_s^2}$$

being the Brunt-Väisälä frequency associated with the hydrostatic state. Our set of equations becoms

$$\begin{aligned} \frac{\partial}{\partial t}\mathbf{u} + (2\vec{\Omega} + \boldsymbol{\zeta}) \times \mathbf{u} &= -\nabla\phi + \phi\frac{\overline{N}^2}{g}\hat{\mathbf{z}} + B\hat{\mathbf{z}} \\ \frac{\partial}{\partial t}\sigma - \frac{1}{\overline{\rho}}\nabla\cdot(\overline{\rho}\mathbf{u}) &= 0 \\ \frac{D}{Dt}(B + \int^z \overline{N}^2) &= 0 \end{aligned} \tag{5.12}$$

(simplifying the mass equation). Note that the simplification of the thermodynamics is only necessary for the third equation; the momentum equation only requires the definition of B which could be viewed as a approximate equation of state $B = B(\theta, S, \overline{p})$.

5.2 — Waves

We can begin to classify kinds of dynamics we expect to see in the ocean by considering waves. If we linearize the dynamics around the hydrostatic state, we have

$$\begin{aligned} \frac{\partial}{\partial t}\mathbf{u} + 2\vec{\Omega}\times\mathbf{u} &= -\nabla\phi + \phi\frac{\overline{N}^2}{g}\hat{\mathbf{z}} + B\hat{\mathbf{z}} \\ \frac{\partial}{\partial t}\frac{B}{g} - \frac{1}{\overline{c_s^2}}\frac{\partial}{\partial t}\phi - \frac{1}{\overline{\rho}}\nabla\cdot\overline{\rho}\mathbf{u} &= 0 \\ \frac{\partial}{\partial t}B &= -\overline{N}^2\mathbf{u}\cdot\hat{\mathbf{z}} \end{aligned} \tag{5.13}$$

5.2.1 — Sound

For high-frequency, small-scale motions, the dominant terms become

$$\frac{\partial}{\partial t}B \simeq 0 \quad , \quad \frac{\partial}{\partial t}\mathbf{u} \simeq -\nabla\phi \quad , \quad \frac{\partial}{\partial t}\phi + \overline{c_s^2}\nabla\cdot\mathbf{u} \simeq 0$$

Combining the last two gives

$$\frac{\partial^2}{\partial t^2}\phi - \overline{c_s^2}\nabla^2\phi = 0$$

This is the classical wave equation (c.f. xx) with c_s giving the characteristic speed of the disturbances. These waves of compression and rarifaction are sound waves. Although we will not deal with these waves, they do offer a simple example to introduce the general nature of wave motion. In particular, we can find a solution like the real part of

$$\phi = A\exp(\imath\Theta(\mathbf{x},t))$$

where the phase function Θ tells us where the maxima ($\Theta = 2n\pi$) and minima ($\Theta = (2n+1)\pi$) are located at any time. For plane waves, $\Theta = \mathbf{k}\cdot\mathbf{x} - \omega t$, so that the peaks and troughs are along planes perpendicular to $\mathbf{k}$. In this form, $\mathbf{k}$ is the wavenumber and ω the frequency.[†] The period is $2\pi/\omega$ and the wavelength is $2\pi/|\mathbf{k}|$. When we put this form in the equations, we get the *dispersion relation*

$$\omega^2 = \overline{c_s^2}|\mathbf{k}|^2$$

The phase speed measures the rate at which the crests and troughs move along some direction; for example, we pick the direction normal to the crests and troughs $\mathbf{k}/|\mathbf{k}|$. The wave now looks like

$$\phi = A\exp\left(\imath\mathbf{k}\cdot\left[\mathbf{x} - c\frac{\mathbf{k}}{|\mathbf{k}|}\right]\right)$$

so that

$$c|\mathbf{k}| = \omega$$

The phase speed is just equal to the speed of soun, $\overline{c_s}$, as promised.

[†] In beginning texts, ω, which has units of radians per second, is called "angular frequency" and "frequency" is reserved for the inverse of the period, measured in Hz or cycles per second. Since ω is the quantity which arises naturally in the equations, we use the simplified wording.

5.2.2 — Inertia-gravity waves

The five linearized equations 5.xx,xx,xx have five time derivatives so we should have five different frequencies given the wavenumber $\mathbf{k}$; sound waves account for two of these ($\pm\overline{c_s}|\mathbf{k}|$) so that we should have three more. These will be motions for which the compressional effects occur only in N^2 and the definition of B. Therefore, we can simplify the mass equation by keeping only the divergence term

$$\nabla \cdot \mathbf{u} = 0 \tag{xxa}$$

and can ignore the N^2/g term in the vertical momentum

$$\frac{\partial}{\partial t}\mathbf{u} + 2\Omega \times \mathbf{u} = -\nabla\phi + B\hat{\mathbf{z}} \tag{xxa}$$

If we assume all variables ar proportional to $\exp(\imath\Theta)$, we can rewrite the equations in matrix form:

$$\begin{pmatrix} -\imath\omega & -f & 0 & \imath k & 0 \\ f & -\imath\omega & 0 & \imath\ell & 0 \\ 0 & 0 & -\imath\omega & \imath m & -1 \\ \imath k & \imath\ell & \imath m & 0 & 0 \\ 0 & 0 & N^2 & 0 & -\imath\omega \end{pmatrix} \begin{pmatrix} u \\ v \\ w \\ \phi \\ B \end{pmatrix} = 0$$

For simplicity, we have made the almost-universal simplification of replacing $2\vec{\Omega}$ by a locally vertical vector $(2\vec{\Omega}\cdot\hat{\mathbf{z}})\hat{\mathbf{z}} = f\hat{\mathbf{z}}$. Since the vertical velocities are much weaker than the horizontal ones, the Coriolis term $[2\vec{\Omega}\cdot\hat{\mathbf{y}}w]\hat{\mathbf{x}}$ is negligible. Likewise the contribution in the vertical momentum $[2\vec{\Omega}\cdot\hat{\mathbf{y}}u]\hat{\mathbf{z}}$ is much smaller than the buoyancy forces. Thus we can usually drop these terms (and must drop both so that the Coriolis force does not alter the energy]; the equatorial region where $f = 0$ can be an exception (c.f., Joyce, 19xx). We shall call this the "f-approximation ." The second part of this approximation involves defining the height above the mean planetary radius a by $r = a + z$ and then dropping order z/a terms. For example, the vertical part of the mass conservation equation becomes

$$\frac{1}{r^2}\frac{\partial}{\partial r}r^2\rho w \quad \rightarrow \quad \frac{1}{(a+z)^2}\frac{\partial}{\partial z}(a+z)^2\rho w \quad \rightarrow \quad \frac{1}{a^2}[a^2\frac{\partial}{\partial z}\rho w + 2a\rho w] \quad \rightarrow \quad \frac{\partial}{\partial z}\rho w$$

The vector $\mathbf{k}$ is written in terms of its components, (k, ℓ, m). This equation will have non-trivial solutions if the determinant vanishes

$$\imath\omega[|\mathbf{k}|^2\omega^2 - N^2(k^2+\ell^2) - f^2m^2] = 0 \tag{5.14}$$

Thus we find the other three frequencies: $\omega = 0$ to be discussed below and the internal waves

$$\omega^2 = \frac{(k^2+\ell^2)N^2 + m^2f^2}{|\mathbf{k}|^2}$$

(if we keep all components of the rotation vector, the $m^2 f^2$ term becomes $|2\vec{\Omega} \cdot \mathbf{k}|^2$.) Unlike sound waves, the frequency depends only on the angle of the wavenumber vector from horizontal ϑ:

$$\omega^2 = N^2 \cos^2 \vartheta + f^2 \sin^2 \vartheta$$

The waves with $\mathbf{k}$ nearly vertical are the low-frequency inertial motions $\omega \sim f$; the motions are nearly horizontal with the parcels moving in clockwise orbits (northern hemisphere). The higher frequency waves have a nearly horizontal $\mathbf{k}$ so that $\omega \sim N$. For these, the motions are nearly vertical, corresponding to buoyancy oscillations. Although these tend to be less energetic than the low-frequency near-inertial motions, they may have more impact on the biota in the surface ocean where vertical motions can alter the light level they experience.

Just as surface waves ride on the density variation between water and air, these internal waves depend on the much weaker density variations within the water column. They are ubiquitous, with a fairly well-defined spectrum (Garrett and Munk, 19xx). In the ocean, internal gravity waves are generated byconvective events, flow over topography, and possibly by the larger scale eddies; rapid wind changes are also an important factor. Experiments (xx, 19xx) have demonstrated that waves with downward propagating energy dominate the upper water column, indicating a surface source.

The phase speed tells us how the peaks and troughs move, but does not represnet the rate at which the energy propagates. For that, we need to consider the *group velocity*

$$\mathbf{c}_g = \frac{\partial \omega}{\partial \mathbf{k}} = \left(\frac{\partial \omega}{\partial k} \, , \, \frac{\partial \omega}{\partial \ell} \, , \, \frac{\partial \omega}{\partial m} \right)$$

Full derivations can be found in many texts; for our purposes, we can justify this form by considering two waves of slightly different wavenumber and frequency:

$$\begin{aligned} \phi &= \cos\left(\left[k + \frac{\delta k}{2} \right] x - \left[\omega + \frac{\delta \omega}{2} \right] t \right) + \cos\left(\left[k - \frac{\delta k}{2} \right] x - \left[\omega - \frac{\delta \omega}{2} \right] t \right) \\ &= 2 \cos\left(\frac{1}{2} [\delta k x - \delta \omega t] \right) \cos(kx - \omega t) \end{aligned}$$

The solution looks like a carrier wave with the crests and troughs moving at $c = \omega/k$ with an envelope modulation. The latter has peaks and nodes with a large-scale separation between the peaks of $2\pi/\delta k$. The envelope moves at speed $c_g = \delta\omega/\delta k$.

For internal waves, surfaces of constant ω in $\mathbf{k}$ space are cones with angle φ from the horizontal. The group velocity, which is the gradient of ω in $\mathbf{k}$ space is perpendicular to these cones and therefore to the wavenumber vector. Therefore upward propagating phase correxponds to downward propagating energy (figure 5.xx). From the dispersion relation

$$\mathbf{c}_g \cdot \hat{\mathbf{z}} = \frac{\partial \omega}{\partial m} = \frac{m}{\omega} \frac{\partial \omega^2}{\partial m^2} = -\frac{m}{\omega} \frac{(N^2 - f^2)(k^2 + \ell^2)}{(k^2 + \ell^2 + m^2)^2}$$

which indeed has the opposite sign from ω/m.

Tidal flows over banks can generate nonlinear internal waves which propagate as a train of "solitons" when the tidal current relaxes (e.g. xx, 19xx, xx, 19xx); these can be seen in acoustic scattering signals, indicating organisms are being moved by the wave currents.

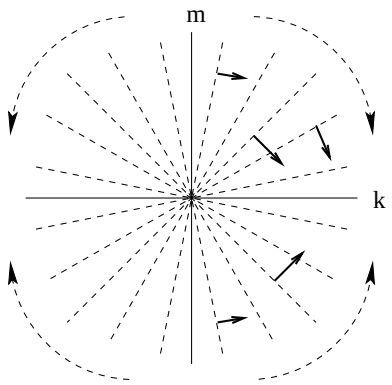

Figure 5.3: Contours of constant ω in the k, m plane (straight dashed lines). The dashed arrows show the direction in which ω is increasing. The solid arrows show the direction of the group velocity.

5.2.3 — Geostrophic waves

Finally, we examine the zero-frequency mode. The equations under the same Boussinesq simplification become

$$2\vec{\Omega} \times \mathbf{u} = -\nabla\phi + B\hat{\mathbf{z}}$$
$$\nabla \cdot \mathbf{u} = 0$$
$$N^2 \mathbf{u} \cdot \hat{\mathbf{z}} = 0$$

The vorticity statement from the first two of these (simplifying 5.xx) gives the general thermal wind statement

$$(2\vec{\Omega} \cdot \nabla)\mathbf{u} = -\frac{1}{\rho^2}\nabla\rho \times \nabla p \simeq \frac{1}{g\rho_0}\nabla B \times \nabla \overline{p} = \hat{\mathbf{z}} \times \nabla B$$

But the set of equations implies a more restricted form, since the thermodynamics indicates that the vertical velocity vanishes; the momentum balnce is then geostrophic

$$u = -\frac{1}{f}\frac{\partial\phi}{\partial y} \quad , \quad v = \frac{1}{f}\frac{\partial\phi}{\partial x}$$

The mass equation is satisfied as long as f is constant, and the third momentum equation just gives

$$2\vec{\Omega} \cdot \nabla\phi = fB \quad ;$$

The thermal wind equations

$$2\vec{\Omega}\cdot\nabla u = -\frac{\partial}{\partial y}B \quad , \quad 2\vec{\Omega}\cdot\nabla v = \frac{\partial}{\partial x}B$$

follow from differentiating and substituting the geostrophic relationships. Under the f-approximation, these reduce to the standard hydrostatic balance and thermal wind formula

$$\frac{\partial\phi}{\partial z} = B \quad , \quad f\frac{\partial}{\partial z}u = -\frac{\partial}{\partial y}B \quad , \quad f\frac{\partial}{\partial z}v = \frac{\partial}{\partial x}B$$

The latter versions are the common forms used in most theoretical studies. Geostrophic calculations from data use the same dynamical balances but keep the full equation of state.†

These flows have associated anomalies in the potential vorticity, unlike sound and gravity waves. To show this, we form the equation for the vertical component of the vorticity

$$\zeta = \frac{\partial v}{\partial x} - \frac{\partial u}{\partial y}$$

by taking the curl of 5.xxa and dotting with $\hat{\mathbf{z}}$:

$$\frac{\partial}{\partial t}\zeta = -\nabla\cdot(f\mathbf{u}) + \frac{\partial}{\partial z}fw$$

For the moment, we treat f as constant and continue with the Boussinesq form of the mass equation; therefore, the first term on the r.h.s. drops out. From the buoyancy equation

$$\frac{\partial}{\partial z}w = -\frac{\partial}{\partial t}\frac{\partial}{\partial z}\frac{B}{N^2}$$

Combining this with the vorticity equation shows us that

$$\frac{\partial}{\partial t}\left[\zeta + f\frac{\partial}{\partial z}\frac{B}{N^2}\right] \equiv \frac{\partial}{\partial t}q' = 0 \tag{5.15}$$

Thus the anomalous potential vorticity q' is conserved. As in the full derivation, the phrase implies that q' includes both the vorticity and other terms which can be traded back and forth with vorticity. In the linearized form here, the

$$\frac{\partial}{\partial z}\frac{B}{N^2}$$

† The general geosterophic-hydrostatic equations with nondivergence of mass flux give

$$(2\vec{\Omega}\cdot\nabla)\rho\mathbf{u} = -\nabla\rho\times\nabla\Phi$$

but we generally calculate in pressure coordinates described in 5.xx.xx) instead.

term measures the thickness between isentropes; i.e., if η is the vertical displacement of an isentrope, then

$$B_{tot}(\mathbf{x}, z+\eta(\mathbf{x},t)) = \int^{z+\eta} N^2 + B(\mathbf{x}, z+\eta, t) = \text{const.} = \int^{z} N^2$$

which becomes

$$N^2\eta + B(\mathbf{x}, z, t) = 0$$

Therefore $\eta \simeq -B/N^2$, and the stretching term is the limit of $-f(\eta_1 - \eta_2)/(z_1 - z_2)$. If a column of fluid between two isentropes is stretched ($\frac{\partial}{\partial z}\eta$ increases) and thereby contracts horizontally, the total spin $f + \zeta$ increases.

We can now differentiate between our fifth lkind of wave and the others: in the dispersion relation 5.xx, the non-zero frequency waves cannot have PV anomalies (since $\omega q' = 0$ from 5.xx, q' must be zero). The motions with signals in the PV are the geostrophic waves or eddies. At the moment, their frequency is zero, but when we move onto the surface of the sphere, where f now depends on a horizontal coordinate, latitude, the frequency becomes non-zero, and the motions correspond to Rossby waves.

The simplest system (within the approximations discussed so far) exhibiting Rossby waves is the barotropic vorticity equation, derived by making the f-and Boussinesq approximations. Since the flow is nondivergent we can represent the velocity as the curl of a vector streamfunction. For the barotropic case, we take

$$\mathbf{u} = -\nabla \times (\psi\hat{\mathbf{z}}) = \hat{\mathbf{z}} \times \nabla\psi$$

where ψ depends only on latitude and longitude. In that case, the vertical velocity is zero, and the buoyancy perturbations vanish. The vertical component of the vorticity is just

$$\zeta = \nabla^2\psi \tag{5.16}$$

Indeed, since the horizontal flows have no vertical shear ($\frac{\partial}{\partial z}\psi = 0$), this is the only non-zero component of the vorticity. To find the evolution of the flow, we look at the vorticity equation

$$\frac{\partial}{\partial t}\nabla \times \mathbf{u} + \nabla \times [(\boldsymbol{\zeta} + f\hat{\mathbf{z}}) \times \mathbf{u}] = 0$$

which becomes

$$\frac{\partial}{\partial t}\zeta + \hat{\mathbf{z}} \cdot \nabla \times [(\zeta + f)\hat{\mathbf{z}} \times \mathbf{u}] = 0$$

Note that we have not linearized. Using the flow–streamfunction relationship gives

$$\frac{\partial}{\partial t}\zeta - \hat{\mathbf{z}} \cdot \nabla \times [(\zeta + f)\nabla\psi] = 0$$

or

$$\frac{\partial}{\partial t}\zeta + \hat{\mathbf{z}} \cdot [\nabla\psi \times \nabla(\zeta + f)] = 0 \quad \text{or} \quad \frac{\partial}{\partial t}\zeta + \mathbf{u} \cdot \nabla(\zeta + f) = 0$$

Thus the potential vorticity $q = \zeta + f$ is conserved

$$\frac{D}{Dt} q = 0 \tag{5.17}$$

The scalar χ here is just the height z which is conserved following the motion since $w = 0$ and satifies the cross-product condition since $B = \int^z dz' N^2(z')$ varies only with z. Equations 5.xx-xx form a closed set: given the vorticity, we can invert the Poisson equation to find ψ and calculate the velocities. Then we can advance the vorticity in time.

For linear waves, we can take the horizontal structure to satisfy

$$\zeta = \nabla^2 \psi = -K^2 \psi \tag{5.18}$$

with K constant. With this form, the nonlinear term $\nabla\psi \times \nabla\zeta$ vanishes, and the dynamics just becomes

$$-K^2 \frac{\partial}{\partial t}\psi + \frac{1}{a^2 \cos\theta} \frac{\partial \psi}{\partial \lambda} \frac{\partial f}{\partial \theta} = 0$$

SInce $f = 2\Omega \sin\theta$, we have

$$\frac{\partial}{\partial t}\psi - \frac{2\Omega}{a^2 K^2} \frac{\partial}{\partial \lambda}\psi = 0$$

Thus the pattern found by solving 5.xx simply propagates westward without change of shape

$$\psi = \psi(\lambda + \frac{2\Omega}{a^2 K^2} t, \theta)$$

To phrase this as a dispersion relation, we can find solutions like

$$\psi \sim F(\theta) \exp(\imath k a \cos\theta_0 \lambda - \omega t)$$

with θ_0 a characteristic latitude, giving

$$\omega = -\frac{\beta k}{K^2} \quad \text{with} \quad \beta = \frac{\partial f}{\partial \theta}\Big|_{\theta_0} = \frac{2\Omega \cos\theta_0}{a}$$

Since $K^2 a^2$ will be large, the propagation speeds will be slow and the periods long. The important parameter is $\beta = |\nabla f|$ which measures the rate at which the planetary vorticity f increases as we go northward. In the barotropic problem where $\zeta + f$ is conserved, northward motion of a parcel of fluid will results in decreaed relative vorticity, while southward motion results in increasing ζ.

Now let us consider the dynamics of these waves. Suppose we have a positive vorticity anomaly; it will have a cyclonic (counter-clockwise in the northern hemisphere) circulation. The streamfunction will be negative in the center (and, if the flow is nearly geostrophic, we will have a low pressure anomaly $p \sim f\psi$). Furthermore, by the nature of solutions of the Poisson equation, ψ will be broader than the anomaly (c.f. figure 5.xx). If we ignore the variations of f, this anomaly can just stay in place. But the β-effect – the fact that f increases with latitude – implies that q has a northward increase in addition to the positive

anomaly. Advection of this gradient tends to increase the vorticity on the left and decrease it on the right. Therefore the anomaly will migrate westward

$$\zeta(t+\delta t) \simeq \zeta(t) + \frac{\partial \zeta}{\partial t}\delta t = \zeta(t) - v\frac{1}{a}\frac{\partial f}{\partial \theta}\delta t = \zeta - \beta v \delta t`$$

But a propagating eddy would have

$$\zeta(t+\delta t) = \zeta(x - c\delta t, y) \simeq \zeta - c\delta t \frac{\partial \zeta}{\partial x}$$

(reverting to a Cartesian notation). Since v looks like $-\frac{\partial \zeta}{\partial x}$, c will be negative and proportional to β. Thus the geostrophic mode no longer has zero frequency, but rather appears as slowly propagating Rossby waves.

Figure 5.4: Inversion of a vorticity anomaly.

5.3 — The beta-plane

The analysis above indicates the important physics associated with the Earth's sphericity resides in the increase in the vertical component of the rotation vector with latitude. If the domain is small enough or if we are doing an idealized study, we often pose the problem in Cartesian coordinates with the only effect of sphericity being represented as a northward increase in $f = f_0 + \beta y$. With the center of the domain at latitude θ_0, the parameters are $f_0 = 2\Omega \sin\theta_0$ and $\beta = 2\Omega \cos\theta_0/a$, and the coordinates are just $y = a(\theta - \theta_0)$, $x = a\cos\theta_0(\lambda - \lambda_0)$. The "beta-plane" equations are simply

$$\frac{D}{Dt}u_i + (f_0 + \beta y)(\hat{\mathbf{z}} \times \mathbf{u})_i = -\frac{1}{\rho}\frac{\partial}{\partial x_i}p + Fric_i$$

$$\frac{\partial}{\partial t}\rho + \frac{\partial}{\partial x_i}\rho u_i = 0$$

$$\frac{D}{Dt}\rho - \frac{1}{c_s^2}\frac{D}{Dt}p = \mathit{Heating/SaltDiffusion}$$

with $\frac{D}{Dt} = \frac{\partial}{\partial t} + u_j \frac{\partial}{\partial x_j}$. As various authors have noted, replacing all the vector operators with Cartesian versions implies that we are dropping some terms of order L/a while retaining the one in the β term. Phillips (19xx) and Verkeley (19xx) give mappings which reproduce the equations above correctly keeping all order one and L/a terms while dropping order L^2/a^2 contributions. In both cases, latitude circles or meridians are no longer straight lines.

We adopt a slightly different approach: if we transform the equations to Mercator coordinates

$$x = a(\lambda - \lambda_0) \quad , \quad y = a \ln\left(\frac{1+\sin\theta}{\cos\theta}\right)$$

The scale factors relating small distances to changes in x or y are the same (as necessary to preserve angles as the map does)

$$dist = \cos\theta \; dx \; , \; \cos\theta \; dy$$

with $\cos\theta = \mathrm{sech}(y/a)$. To order $(y/a)^2$, the scale factors are just one, so that the curl, gradient, and divergence look just like the Cartesian versions. But the vertical component of the rotation

$$f = 2\Omega \sin\theta = 2\Omega \tanh(y/a) \simeq \frac{2\Omega}{a} y$$

The equations become the "equatorial beta-plane" system, with $f_0 = 0$ and β given by the value at the equator.

If we accept these and recenter the $y = 0$ line to be some other latitude, we recover the ordinary beta-plane equations. In principle, we are still bound by the restriction that the northern and southern latitudes should be less than about 50^o where $y = a$; in practice, we ignore this restriction for process studies and use spherical coordinates when more realism is desired.†

5.4 — Approximations to the equations of motion

When we solve the equations of motion, either analytically or numerically, we have a range of space and time scales which we are really interested in. To make progress, we end up filtering out motions which are outside those ranges. By removing fast, but uninteresting, waves, we can much more readily apply numerical methods. Advection algorithms are limited by the CFL condition

$$U\delta t < \text{const. } \delta x$$

where U is a characteristic flow or wave speed (see appendix xx): the time step is limited by the fastest speeds. If we are not interested in acoustic waves movint at 1500 m/s, we should work with equations which have filtered them out.

† We can obtain the ordinary beta-plane equations by rotating the sphere so that the desired center point is at the equator and then projecting; again the latitude circles and meridians will be curved.

5.4.1 — Anelastic and Boussinesq equations

We begin by removing the sound waves. The anelastic equations (c.f. Ingersoll, 2005) do this while retaining the large density variations from top to bottom, the compressible form of N^2, and the potential for thermobaric instability. We follow the same steps introduced in the discussion of the hydrostatic state (5.xx.xx) but choose an isentropic, constant salinity background. To indicate the adiabatic nature, we shall use a subscript "a" rather than the overbar. We assume that the density can be written as a function of potential temperature, salinity and pressure $\rho(\theta, S, p)$; Wright (1997) and McDougall *et al.*(2003), JAOT provide explicit formulae for density in terms of these variables. We define a uniform salinity S_a and potential temperature θ_a background; from these we can find the background temperature $T_a(p)$ and density $\rho_a(p)$; with the hydrostatic relation, we can reinterpret the latter to give $\rho_a(z)$ and $p_a(z)$. But now the Brunt-Väisälä freqency associated with this state is

$$N_a^2 = g^2 \rho_a [K(\theta_a, S_a, p_a) - K_a] = 0$$

Therefore the momentum equations become

$$\frac{\partial}{\partial t}\mathbf{u} + (f\hat{\mathbf{z}} + \nabla \times \mathbf{u}) \times \mathbf{u} = -\nabla\phi - \nabla\frac{1}{2}|\mathbf{u}|^2 + B\hat{\mathbf{z}} \tag{5.19}$$

with $B = g(\sigma + \rho_a K_a \phi)$. But, with the definition

$$\ln(1+\sigma) \simeq \sigma = \ln\rho(\theta_a, S_a, p_a) - \ln\rho(\theta_a + \theta', S_a + S', p_a + \rho\phi)$$

we can Taylor expand just the last part to find

$$\sigma \simeq \ln\rho_a - \ln\rho(\theta, S, p_a) - \rho_a \phi K_a$$

so that the buoyancy takes the simpler form

$$B = g \ln\frac{\rho_a}{\rho(\theta, S, p_a)} = B(\theta, S, z) \tag{5.20}$$

The thermodynamic equations just reduce to the potential temperature statement

$$\frac{D}{Dt}\theta' = -\frac{\theta_a}{T_a c_{p_a}} \nabla \cdot \mathbf{Q} \tag{5.21}$$

and the salt equation is unchanged. We close the system with the simplified mass equation

$$\nabla \cdot \rho_a \mathbf{u} = 0 \tag{5.22}$$

Since the density changes induced by compression have been dropped, sound waves no longer appear in the anelastic system 5.xx-xx.

As Ingersoll points out in the special case with $B/g = \alpha(z)\theta' - \beta(z)S'$, they do retain conservation of energy, and the statement still holds when we include more terms in the

Tayloir series expansion of B. Gravity and Rossby waves remain, as do convection and turbulence.

For theoretical work, we can again use the simplified thermodynamics 5.xx to replace the potential temperature and salinity equations with a buoyancy conservation statement

$$\frac{D}{Dt}B = -\nabla \cdot \mathbf{Q}_B \tag{5.23}$$

where the buoyancy fluxes $\mathbf{Q}_B$ include heating and salinity changes as well as diffusive transport.

The Boussinesq equations can be regarded as a further simplification in which ρ_a is taken to be constant and the explicit depth variation of B associated with p_a is ignored. The ρ_a variations of a few percent seem to have quantitative, but not qualitative effects (and we can scarcely expect our other errors to be as small in any case, although this one will be systematic). The approximation $B(\theta', S', p_a) = B(\theta', S')$ is not terribly accurate, but again can be very useful for gaining insight into dynamical processes where θ and S cannot just be combined into a buoyancy (e.g. double diffusion). The buoyancy is advected, but the non-conservative terms

$$\frac{D}{Dt}B = -g\frac{\partial B_a}{\partial \theta'}\frac{D}{Dt}\theta' - g\frac{\partial B_a}{\partial S'}\frac{D}{Dt}S' = g\frac{\partial B_a}{\partial \theta'}\frac{\theta_a}{T_a c_{p0}}\nabla \cdot \mathbf{Q} - g\frac{\partial B_a}{\partial S'}SaltDiffusion$$

may require separate knowledge of θ' and S'. As in Chapter 1 and 5.xx, we can often approximate the nonconservative terms by diffusion of buoyancy plus external heating/ freshening. For laboratory systems where the equation of state can be regarded as linear and the components mix similarly (turbulent diffusion), such an approximation is quite adequate; for the ocean, we will miss phenomena such as caballing which rely on the curvature in the density contours on a TS plot so that fluid formed by mixing two water masses can be heavier than either parent. Perhaps the real message is that approximations such as these produce simpler equation sets which allow us to make tremendous progress on many problems but can lead us astray in a few cases becuase they are missing some complexities of the full system. I will continue to use these (and the following) filtered equation systems with the expectation that they capture the important parts of the physics.

5.4.2 — Boundary conditions

To complete the specification of the dynamics, we must define conditions at the bottom, top, and sides. These state that the surfaces are impenetrable; for solid walls or bottom topography

$$\mathbf{u} \cdot \hat{\mathbf{n}} = 0$$

where $\hat{\mathbf{n}}$ is the unit normal to the surface. For bottom topography at $z = -H(x, y)$, this can also be written as $\frac{D}{Dt}(z + H) = 0$ which implies

$$w(x, y, -H) = -\frac{D}{Dt}H(x, y)\big|_{z=-H}$$

The upper surface $z = \eta(x, y, t)$ has the additional complication of being free to move; however, the condition can be expressed similarly as

$$\frac{D}{Dt}(\eta - z) = 0 \quad \Rightarrow \quad \frac{D}{Dt}\eta\big|_{z=\eta} = w(x, y, \eta, t)$$

In addition, we must match the normal forces (pressure) across the sea surface

$$p(x, y, \eta, t) = p_{at}$$

with p_{at} being the atmopheric pressure. In the anelastic case, this becomes

$$p_a(\eta) + \rho_a \phi(x, y, \eta, t) = p_{at}$$

Unless we are concerned with nonlinear surface gravity waves, we can linearize these two expressions (since the characteristic sea-surface elevation is rarely more than a meter on scales of kilometers)

$$[\frac{\partial}{\partial t} + \mathbf{u}_h(x, y, 0, t) \cdot \nabla]\eta(x, y, t) = w(x, y, 0, t)$$

$$\phi(x, y, 0, t) = g\eta + \frac{1}{\rho_a(0)} p_{at}$$

These conditions (except for the pressure matching) are called kinematic conditions because they simply express the fact that the surface is a boundary through which fluid does not pass. Strictly speaking, evaporation and precipitation violate that precept; Huang (19xx-xx) has argued for treating the freshwater balance and salt balance separately incorporating the sources and sinks of water explicitly rather than regarding precipitation as just decreasing the salinity. For most of our problems, the effects will be minor.

When non-conservative effects are included, we will also need to specify the viscous/ diffusive fluxes of momentum and buoyancy across the boundary. The equations discussed so far can include atmospheric pressure variations and penetrative heating as forcing mechanisms for oceanic motions; however, wind stresses and buoyancy forcing at the surface (IR radiation and evaporation/ precipitation) must be included in any basin or global scale model as well as being significant in many local problems. Indeed, the upwelling example in Chapter 1 demonstrated the importance of wind stress in the coastal areas. Other forcing mechanisms such as tides or geothermal heating may also impact the circulation being considered.

We shall, therefore, supplement the kinematic boundary conditions with wind stresses

$$\nu \frac{\partial}{\partial z}\mathbf{u}_h = \tau_w/\rho_a(0)$$

and surface heating and evaporation/ precipitation

$$\kappa \frac{\partial}{\partial z}\theta = Q_a/\rho_a c_p \quad , \quad \kappa \frac{\partial}{\partial z} S = E - P$$

Note the reverse sign convention: we generally talk of vertical fluxes as upward transfers; here the forcing terms represent downwards transfer into the ocean.

5.4.3 — Hydrostatic (primitive) equations

Most models for the meso- and large-scale motions ignore the vertical accelerations in comparison to buoyancy forces. Scale estimates justify this approximation when the horizontal scale L is larger than the vertical one H. The mass equation implies $w \sim uH/L$, and the horizontal momentum suggests that $\phi \sim fuL$ or u^2. Then $\frac{D}{Dt}w \sim uw/L = u^2H/L^2$ will be order $(u/fL)H^2/L^2$ or H^2/L^2 compared to $\frac{\partial}{\partial z}\phi$. We then arrive at the so-called "primitive equations" which can be written as

$$\begin{aligned}
\frac{\partial}{\partial t}\mathbf{u}_h + (f\hat{\mathbf{z}} + \nabla \times \mathbf{u}_h) \times \mathbf{u} &= -\nabla_h(\phi + \frac{1}{2}|\mathbf{u}_h|^2) + \textit{Friction} \\
\frac{\partial}{\partial z}\phi &= B(\theta', S', z) \\
\nabla \cdot \rho_a \mathbf{u} &= 0 \\
\frac{D}{Dt}\theta' &= \textit{Heating} \\
\frac{D}{Dt}S' &= \textit{SaltDiffusion}
\end{aligned}$$

with the h subscript indicating only the horizontal parts of the vector or operator are included.

These equations badly misrepresent convective processes, so that density-driven overturning is usually handled by convective adjustment in which unstable pairs of vertical gridpoints with

$$N^2 = \frac{\partial B}{\partial z} < 0$$

are averaged until N^2 is everywhere non-negative. In addition, by design, the frequencies of short waves (internal or surface) will be off.

But the approximation has a significant advantage as well; to see this, recall that the pressure in the Boussinesq approximation had no prognostic equation but needed to be calculated diagnostically as the term required to maintain volume conservation. To apply to the anelastic equations, we multiply the momentum equations by ρ_a and take the divergence:

$$\nabla \cdot [\rho_a(f\hat{\mathbf{z}} + \boldsymbol{\zeta}) \times \mathbf{u}] = -\nabla \cdot \rho_a \nabla(\phi + \frac{1}{2}|\mathbf{u}|^2) - \nabla \cdot [\rho_a \sigma_a \nabla \Phi]$$

Another way to think about the procedure is as a correction step: we find velocity changes without the Bernouilli function

$$\frac{\partial}{\partial t}\tilde{\mathbf{u}} = -(f\hat{\mathbf{z}} + \boldsymbol{\zeta}) \times \mathbf{u} - \sigma_a \nabla \Phi$$

and then correct the acceleration

$$\frac{\partial}{\partial t}\mathbf{u} = \frac{\partial}{\partial t}\tilde{\mathbf{u}} - \nabla \phi_B$$

with $\phi_B = \phi + \frac{1}{2}|\mathbf{u}|^2$ found from

$$\nabla \cdot \rho_a \nabla \phi_B = \nabla \cdot \rho_a \frac{\partial}{\partial t} \tilde{\mathbf{u}}$$

In any case, we must solve a three-dimensional Laplace-like equation for the Bernouilli function.

Primitive equation models which resolve the free surface have no such difficulty: our state vector ($\mathbf{u}_h$, η, θ, S) has the information required to step the system forward. From the surface elevation, we find $\phi(x, y, 0) = g\eta$; the hydrostatic equation can be integrated to give $\phi(x, y, z)$. From $\mathbf{u}_h$ and the nottom boundary condition, we can compute w using the mass equation

$$\frac{1}{\rho_a} \frac{\partial}{\partial z} \rho_a w = -\nabla_h \cdot \mathbf{u}_h$$

We now have everything required to evaluate $\frac{\partial}{\partial t}$ of the state variables.

Unfortunately, the simplicity in the above approach comes at a substantial cost: because of the free surface, we will have long gravity waves propagating at a speed $\sqrt{gH}$ which is on the order of 200 m/s, much larger than the few meters per second speeds of the internal waves. Correspondly, we need a much smaller time step. Split time steps, in which the gravity waves are advanced using many short steps while the baroclinic and vortical fields are adjusted with a much larger δt, can be used to alleviate the problem.

As an alternative, modellers use the "rigid lid approximation" which replaces the kinematic upper boundary condition by $w = 0$. As in the anelastic model, we enforce the conservation of mass at the next time-step and thereby determine the unknown pressure $\phi(x, y, 0)$ (or, equivalently, η). We can now write the conservation of mass in an integrated form

$$\nabla_h \cdot \int_{-H}^{0} \mathbf{u}_h = 0$$

This comes from using

$$\frac{\partial}{\partial x} \int_a^b u = \int_a^b \frac{\partial}{\partial x} u + u(b) \frac{\partial}{\partial x} b - u(a) \frac{\partial}{\partial x} a \quad \Rightarrow$$

$$\nabla_h \int_{-H}^{0} \mathbf{u}_h = \int_{-H}^{0} \nabla_h \cdot \mathbf{u}_h + \mathbf{u}(-H) \cdot \nabla H = w(-H) + \mathbf{u}(-H) \cdot \nabla H = 0$$

Suppose we define the baroclinic pressure

$$\frac{\partial}{\partial z} \phi_{bc} = B \quad , \quad \phi(x, y, 0, t) = 0$$

and the first estimate of the acceleration

$$\frac{\partial}{\partial t} \hat{\mathbf{u}}_h = -(f \hat{\mathbf{z}} + \boldsymbol{\zeta}_h) \times \mathbf{u} - \nabla \phi_b + \mathit{Fric}$$

Then the actual acceleration is given by

$$\frac{\partial}{\partial t}\mathbf{u}_h = \frac{\partial}{\partial t}\hat{\mathbf{u}}_h - \nabla\phi_s \quad , \qquad \phi_s = \phi(x, y, 0, t)$$

and conservation of mass implies that

$$\int_{-H}^{0} \nabla \cdot \frac{\partial \hat{\mathbf{u}}_h}{\partial t} = \nabla \cdot H\nabla\phi_s$$

which is a 2D Laplace-like equation for the surface pressure. Solving this is a much smaller job than solving the full 3D problem, so that the primitive equations can be time-stepped more readily (Marshall, 19xx, does argue that splitting the pressure into the hydrostatic, surface, and non-hydrostatic parts leads to a fairly small cost for finding the third part).

Finally, we note that the hydrostatic assumption, applied *ab initio*, allows us to avoid the anelastic/ Boussinesq approximation by using some function of pressure $\xi(p)$ as the vertical coordinate. This old idea from meteorology filtered into oceanography (at least in joint courses!); DeSzoeke and Samelson (2002) give a good summary for $\xi = p$; we have preferred to use the more general form and define

$$\frac{\partial p}{\partial \xi} = -\rho_c(\xi)g$$

We skip the derivations; the equations become

$$\begin{aligned}
\frac{\partial}{\partial t}\mathbf{u}_h + (f\hat{\mathbf{z}} + \boldsymbol{\zeta}_h) \times \mathbf{u} &= -\nabla\varphi + B\hat{\mathbf{z}} \\
\nabla_h \cdot \mathbf{u}_h + \frac{1}{\rho_c}\frac{\partial}{\partial \xi}\rho_c\omega &= 0 \\
\frac{\partial}{\partial t}B + \mathbf{u}_h \cdot \nabla_h B + \omega\tilde{N}^2 &= 0
\end{aligned}$$

with

$$\omega = \frac{D}{Dt}\xi$$

the effective vertical velocity and

$$\frac{D}{Dt} \to \frac{\partial}{\partial t} + u\frac{\partial}{\partial x} + v\frac{\partial}{\partial y} + \omega\frac{\partial}{\partial \xi}$$

The pressure is replaced by the geopotential $\phi = gz(x, y, \xi, t)$, the buoyancy is $B = g\rho_c/\rho$, and

$$\tilde{N}^2 = \frac{\partial B}{\partial \xi} - B\frac{\partial \ln \rho_c}{\partial \xi} - \frac{1}{c_s^2}B^2$$

is $(\rho_c/\rho)^2 = B^2/g^2$ times the standard N^2. At the surface (without atmospheric forcing), the kinematic boundary conditions are simple

$$\phi(\mathbf{x}_h, 0) = g\eta \quad , \quad \omega(\mathbf{x}_h, 0) = 0$$

while at the bottom they become more complex

$$\phi(\mathbf{x}_h, \xi_b(\mathbf{x}, t), t) = -gH(x, y) \quad , \quad \omega(\mathbf{x}_h, \xi_b, t) = \left[\frac{\partial}{\partial t} + \mathbf{u}_h(\mathbf{x}_h, \xi_b, t) \cdot \nabla\right] \xi_b$$

We recover systems similar to the Boussinesq or anelastic hydrostatic equations by choosing ρ_c to be constant or $\rho_a(p)$ respectively; however, the boundary conditions are more complex.

5.4.4 — Quasigeostrophic equations and relatives

As a final approximation, we discuss the large-scale, nearly geostrophic flows; the filtering here removes gravity waves. We could use a number of approaches here, but shall choose one which illustrates the connections to Rossby waves with their potential vorticity anomalies. We begin with the conservation of PV for the hydrostatic, anelastic equations

$$\frac{D}{Dt} q = 0 \quad , \quad q = \frac{1}{\rho_a}(f\hat{\mathbf{z}} + \nabla \times \mathbf{u}_h) \cdot \nabla\chi$$

where χ is a scalar field which is conserved and which satisfies

$$\hat{\mathbf{z}} \cdot (\nabla\chi \times \nabla B) = 0$$

This requirement (which appears as

$$\nabla\chi \cdot (\nabla\rho \times \nabla p) = 0$$

in the full equation set) is non-trivial; for single component fluids with $\rho = \rho(\theta, p)$, we can use $\chi = \theta$, but this will not work when ρ also depends on salinity. We shall use the simplified thermodynamics approximation in which B itself is conserved, so that $\chi = B$. Thus the potential vorticity

$$q = \frac{1}{\rho_a}(f\hat{\mathbf{z}} + \boldsymbol{\zeta}_h) \cdot \nabla B \tag{5.24}$$

is conserved in adiabatic frictionless flow.

A bit of calculation using the hydrostatic equation shows us that

$$\begin{aligned}
N^2 &= -g\frac{\partial}{\partial z}\ln\rho + gK_a\frac{\partial}{\partial z}p \\
&= -g\frac{\partial}{\partial z}\ln\rho_a + g\frac{\partial}{\partial z}\ln(1+\sigma) + g\left(-g\rho_a + \frac{\partial}{\partial z}\rho\phi\right)K_a(p_a+\rho\phi) \\
&\simeq -g\frac{\partial}{\partial z}\ln\rho_a - g^2\rho_a K_a(p_a) + g\frac{\partial}{\partial z}\sigma - g^2\rho_a\frac{\partial K_a}{\partial p}\rho_a\phi + gK_a(p_a)\frac{\partial}{\partial z}\rho_a\phi \\
&= g\frac{\partial}{\partial z}\sigma + g\rho_a\phi\frac{\partial}{\partial z}K_a(p_a) + gK_a(p_a)\frac{\partial}{\partial z}\rho_a\phi \\
&= \frac{\partial}{\partial z}[g\sigma + g\rho_a\phi K_a] \\
&= \frac{\partial}{\partial z}B
\end{aligned}$$

to the first order in deviations of density and pressure from the isentropic state.

QUASIGEOSTOPHIC

For the quasigeostrophic (QG) system, two parameters, the Rossby number $\epsilon = U/fL$ and the beta number $\beta L/f$, are assumed to be small while the stratification parameter NH/fL is taken to be order one. We split $B = \overline{B}(z) + B'(\mathbf{x},t)$ and connect the Brunt-Vaisala frequency to the large-scale mean

$$N^2 = \frac{\partial}{\partial z}\overline{B}$$

The horizontal velocities are close to the geostrophic value

$$\mathbf{u}_h \simeq \frac{1}{f}\hat{\mathbf{z}}\times\nabla\phi \simeq \hat{\mathbf{z}}\times\nabla\frac{\phi}{f} \equiv \hat{\mathbf{z}}\times\nabla\psi$$

We can use the fact that

$$\hat{\mathbf{z}}\times\nabla\psi = -\nabla\times\psi\hat{\mathbf{z}}$$

for the coordinate systems of interest to see that the horizontal flow is, for small Rossby number and beta parameter, the curl of a vector fields and is nondivergent

$$\mathbf{u}_h = -\nabla\times\psi\hat{\mathbf{z}}$$

To this order, the horizontal advection of a scalar becomes

$$\frac{D_h}{Dt}Q = \frac{\partial}{\partial t}Q + (\hat{\mathbf{z}}\times\nabla\psi)\cdot\nabla Q = \frac{\partial}{\partial t}Q + \hat{\mathbf{z}}\cdot(\nabla\psi\times\nabla Q) \tag{5.25}$$

but we shall continue to use the D_h/Dt notation. The vorticity is just

$$\boldsymbol{\zeta} = \nabla\times\mathbf{u}_g = \nabla^2\psi\hat{\mathbf{z}} - \nabla(\nabla\cdot\psi\hat{\mathbf{z}}) = \hat{\mathbf{z}}\nabla_h^2\psi - \nabla_h\frac{\partial\psi}{\partial z}$$

and the buoyancy becomes

$$B' = f\frac{\partial}{\partial z}\psi$$

The potential vorticity, including terms of relative order 1, Rossby number and beta number, is

$$q \simeq N^2\left[f + \nabla_h^2\psi + f^2\frac{1}{\rho_a N^2}\frac{\partial}{\partial z}\rho_a\frac{\partial}{\partial z}\psi\right]$$

The buoyancy equation

$$f\rho_a\frac{D_h}{Dt}\frac{\partial}{\partial z}\psi + w\rho_a N^2 = 0 \quad \text{or} \quad \frac{D_h}{Dt}\frac{\partial}{\partial z}\psi + w\frac{N^2}{f} = 0 \tag{5.26}$$

allows us to rewrite the PV equation as

$$\frac{D_h}{Dt}\left[f + \nabla_h^2\psi + f^2\frac{1}{\rho_a N^2}\frac{\partial}{\partial z}\rho_a\frac{\partial}{\partial z}\psi - \frac{f^2}{N^4}\frac{\partial N^2}{\partial z}\frac{\partial}{\partial z}\psi\right] = 0$$

or

$$\frac{D_h}{Dt}\left[f + \nabla_h^2\psi + \frac{1}{\rho_a}\frac{\partial}{\partial z}\frac{\rho_a f^2}{N^2}\frac{\partial}{\partial z}\psi\right] = 0$$

Since the horizontal advection can be written (to the relevant order) in terms of the streamfunction (eqn. 5.xx), we have the dynamics expressed in terms of a single scalar field ψ with the QG-PV

$$Q = f + \nabla_h^2\psi + \frac{1}{\rho_a}\frac{\partial}{\partial z}\frac{\rho_a f^2}{N^2}\frac{\partial}{\partial z}\psi$$

being conserved following the horizontal geostrophic flow.

From a time-stepping perspective, we think of Q as the fundamental scalar and invert (solve) the Poisson-like equation 5.xx to find ψ given the PV field. However, solving

$$\left[\nabla_h^2 + \frac{1}{\rho_a}\frac{\partial}{\partial z}\frac{\rho_a f^2}{N^2}\frac{\partial}{\partial z}\right]\psi = Q - f \equiv Q' \tag{5.27}$$

requires boundary conditions at the top and bottom. At the sea-surface, we can specify the buoyancy

$$B'_s(\mathbf{x}_h, t) = f\frac{\partial}{\partial z}\psi(\mathbf{x}_h, 0, t);$$

dynamically, this quantity is conserved, since $w = 0$ at $z = 0$, so that we can step it forward in time

$$\frac{D_h}{Dt}B_s = 0$$

At the bottom, we can combine the kinematic condition

$$w = -\frac{D_h}{Dt}H$$

with the buoyancy equation to find

$$\frac{D_h}{Dt}\left[\frac{\partial}{\partial z}\psi - \frac{N^2 H}{f}\right] = 0$$

Scaling indicates that the depth variations should be order Rossby number so that this can be applied at the mean depth rather than the local one. But the real requirement is just that the vertical velocity must remain small enough so that the horizontal divergence remains order Rossby or beta number.

Vertical velocity

The vertical velocity is important for biological problems, but is not solved explicitly in 5xx-xx. We can derive a diagnostic equation for w by considering the vorticity equation together with the buoyancy equation 5.xx. We take the curl of the momentum equations and look at the vertical component. From Appendix xx, we see that the vorticity changes according to

$$\frac{\partial}{\partial t}\zeta + \nabla_h \cdot [\mathbf{u}(\zeta + f)] - \nabla_h \cdot [w\boldsymbol{\zeta}] = 0$$

Therefore

$$\frac{D_h}{Dt}(\zeta + f) = (f + \zeta)\frac{1}{\rho_a}\frac{\partial}{\partial z}\rho_a w + \nabla_h \cdot w\boldsymbol{\zeta}$$

Within the QG approximation, the last term on the right and the ζ term can be neglected, giving

$$\frac{D_h}{Dt}(\zeta + f) = f\frac{1}{\rho_a}\frac{\partial}{\partial z}\rho_a w$$

implying that vertical vorticity or changes in planetary vorticity result for stretching or squashing of the total vorticity (which is dominated by f). The QGPV equation follows from eliminating w between this equation and 5.xx. The so-called "omega equation" comes from differentiating the vorticity equation with repect to z and subtracting the Laplacian of the buoyancy equation:

$$f^2\frac{\partial}{\partial z}\frac{1}{\rho_a}\frac{\partial}{\partial z}\rho_a w + N^2\nabla^2 w = f\frac{\partial}{\partial z}[\mathbf{u}_h \cdot \nabla(\nabla^2\psi + f)] - f\nabla^2[\mathbf{u}_h \cdot \nabla\frac{\partial}{\partial z}\psi]$$

Note that some terms will cancel, but, in essence, vertical velocities act to maintain the thermal wind balance against the advection of vorticity and of buoyancy.

To see this in more detail, consider a system like the upwelling region in Chapter xx – flow independent of y. The fluid can still have nonzero y-directed velocity v and vorticity ζ_y. The latter satisfies

$$\frac{\partial}{\partial t}\zeta_y + \mathbf{u} \cdot \nabla\zeta_y = f\frac{\partial}{\partial z}v - \frac{\partial}{\partial x}B \tag{5.28}$$

(in the Boussinesq case). If we consider a state with sloping isopycnals having lighter water to the east, but no meridional velocity, a flow in the x-z plane will develop with the light water upwelling and the denser water downwelling. This decreases $\frac{\partial}{\partial x}B$ and, at the same

time (from $\frac{\partial}{\partial t}v = fu$), builds up northtward velocities in the uppser ocean and southward flows in the deep. Thus $\frac{\partial}{\partial z}v$ increases; both of the changes reduce the imbalance in the thermal wind. The vorticity generation term vanishes when thermal wind is restored. If we create the situation above (or make some instantaneous disruption of balance), we would expect to overshoot the balanced state and oscillate. However, when the forces that throw the system out of balance act slowly compared to the periods of these internal gravity waves, the fluid will change slowly maintaining near balance at all times. The vertical velocity (and the implied weak divergent horizontal flows) reconcile the changes and the state of geostrophic/ hydrostatic balance.

Planetary geostrophy

When the scale becomes larger, the beta number becomes order one, while the Rossby number becomes very small. In this limit, the geostrophic and hydrostatic approximations become quite good

$$\mathbf{u}_h = -\frac{1}{f}\nabla \times \phi\hat{\mathbf{z}} \quad , \qquad \frac{\partial}{\partial z}\phi = B$$

The mass conservation equation gives

$$\nabla \cdot \mathbf{u}_h = -\nabla \cdot \left[\frac{1}{f}\nabla \times \phi\hat{\mathbf{z}}\right] = \frac{\nabla f}{f^2} \cdot \nabla \times \phi\hat{\mathbf{z}} = -\frac{1}{f}\nabla f \cdot \mathbf{u}_h = -\frac{1}{\rho_a}\frac{\partial}{\partial z}\rho_a w$$

which is the Sverdrup balance

$$\beta v = f\frac{1}{\rho_a}\frac{\partial}{\partial z}\rho_a w$$

or

$$\frac{1}{\rho_a}\frac{\partial}{\partial z}\rho_a w = \nabla\phi \cdot \left[\frac{\nabla f \times \hat{\mathbf{z}}}{f^2}\right]$$

Thus we can express all three components of the velocity given the pressure (and the value of w at some depth).

The dynamics appears in the buoyancy equation

$$\frac{D}{Dt}B = 0$$

From ϕ, we can calculate $\mathbf{u}$ and B and then advance B in time. With a second suitable boundary condition, we can then calculate ϕ at the new time. For example, consider waves on the sphere in this system. Linearizing the buoyancy equation gives

$$w = -\frac{\partial}{\partial t}\frac{f}{N^2}\frac{\partial}{\partial z}\phi$$

so that

$$\frac{\partial}{\partial t}\left[\frac{1}{\rho_a}\frac{\partial}{\partial z}\frac{\rho_a f^2}{N^2}\frac{\partial}{\partial z}\right]\phi = -\frac{1}{a}\frac{\partial f}{\partial \theta}\frac{1}{a\cos\theta}\frac{\partial}{\partial \lambda}\phi = -\frac{2\Omega}{a^2}\frac{\partial}{\partial \lambda}\phi$$

The vertical operator is the same as that in the quasigeostrophic equations and in the eqations for hydrostatic waves in general; we can separate variables locally and solve

$$\left[\frac{1}{\rho_a}\frac{\partial}{\partial z}\frac{\rho_a}{N^2}\frac{\partial}{\partial z}\right]\phi = -\gamma^2\phi \quad , \qquad \frac{\partial}{\partial z}\phi = 0 \;\; @ \;\; z = 0, -H$$

The eigenvalue is related to the long internal gravity wave speed by

$$c_{gw} = \pm 1/\gamma$$

or to the Rossby deformation radius

$$R_d = (\gamma f)^{-1} = c_{gw}/f$$

The meaning of the former is obvious; the deformation radius applies to geostrophic flows and gives the horizontal scale of response to a baroclinic perturbation. For example, if we have an anomaly of QG PV

$$Q' = \Delta\delta(x - x_a)F(z)$$

where $F(z)$ is the eigenfunction of

$$\frac{1}{\rho_a}\frac{\partial}{\partial z}\frac{\rho_a f^2}{N^2}\frac{\partial}{\partial z}F = -\gamma^2 F \quad , \qquad \frac{\partial}{\partial z}F = 0 \;\; @ \;\; z = 0, -H$$

(typically positive in the upper water and negative below the thermocline), the geostrophic streamfunction is

$$\psi = -\frac{1}{2}\Delta R_d \exp(-|x - x_a|/R_d)$$

which decays over a length equal to the deformation radius.

We can now find a solution for the planetary scale waves

$$\phi = \phi_a F(z)\exp(\imath m\lambda - \imath\omega t)$$

with

$$\omega = -2\Omega m\frac{R_d^2}{a^2}$$

Note that this is really a local result: we have no reason to expect R_d to be constant, and, indeed, calculations of it (c.f. Chelton, *et al.*,1998) show $R_d \sim H/f$. Correspondingly, if we think of the local x-wavenumber as being $m = k * a * \cos\theta$, then

$$\omega = -\beta k R_d^2 \quad \Rightarrow \quad c = -\beta R_d^2$$

with $\beta = 2\Omega\cos\theta/a = |\nabla f|$

5.5 — Layered/ isopycnal models

As Veronis pointed out in 19xx, models in x, y, z coordinates can have unrealistically strong mixing across isopycnal surfaces when these are slanted, since horizontal fluxes project onto cross-isopycnal fluxes. The common approach of using horizontal ν and κ's which are larger than the vertical ones compounds the error (see appendix xx for reasons). To control or even eliminate fluid mixing across density surfaces, we can reformulate the hydrostatic system as a series of stacked layers with different densities (ignoring compressibility).

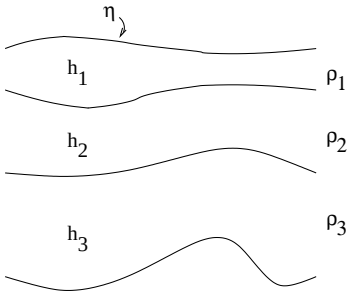

Figure 5.5: layer model

The pressures in the top, second, third, and n^{th} layers are given by

$$\begin{aligned}
\frac{p_1}{\rho_1} &= g(\eta - z) \\
\frac{p_2}{\rho_2} &= g\frac{\rho_1}{\rho_2}h_1 + g(\eta - h_1 - z) \\
&= g(\eta - z) - g\frac{\rho_2 - \rho_1}{\rho_2}h_1 \\
\frac{p_3}{\rho_3} &= g(\eta - z) - g\frac{\rho_3 - \rho_1}{\rho_3}h_1 - g\frac{\rho_3 - \rho_2}{\rho_3}h_2 \\
\frac{p_n}{\rho_n} &= g(\eta - z) - g\sum_1^{n-1}\frac{\rho_n - \rho_j}{\rho_n}h_j
\end{aligned}$$

or, in terms of the ϕ which contains the horizontally varying part of the pressure,

$$\begin{aligned}
\phi_1 &= g\eta \\
\phi_2 &= \phi_1 - g\frac{\rho_2 - \rho_1}{\rho_2}h_1 \\
\phi_3 &= \phi_1 - g\frac{\rho_3 - \rho_1}{\rho_3}h_1 - g\frac{\rho_3 - \rho_2}{\rho_3}h_2 \\
\phi_n &= \phi_1 - g\sum_1^{n-1}\frac{\rho_n - \rho_j}{\rho_n}h_j
\end{aligned} \tag{5.29}$$

Within each layer, the density is constant, so the horizontal velocities can be taken to be independent of depth, although they vary from layer to layer. For large scales, the thermal wind balance mandates $\frac{\partial}{\partial z}u_n = \frac{\partial}{\partial z}v_n = 0$, but in any case it is consistent in that flows independent of depth will not develop shear. The horizontal vorticities are zero and remain zero. Therefore, the momentum equations take the simple form

$$\frac{\partial}{\partial t}\mathbf{u} + (\zeta + f)\hat{\mathbf{z}} \times \mathbf{u} = -\nabla(\phi + \frac{1}{2}|\mathbf{u}|^2) \tag{5.30}$$

with $\mathbf{u}$ the horizontal velocity and $\zeta = \hat{\mathbf{z}} \cdot \nabla \times \mathbf{u}$ the vertical component of vorticity. The vertical velocity, w, is piecewise linear since

$$\nabla \cdot \mathbf{u} + \frac{\partial}{\partial z}w = 0 \quad \Rightarrow \quad \nabla \cdot \frac{\partial \mathbf{u}}{\partial z} + \frac{\partial^2 w}{\partial z^2} = 0 \quad \Rightarrow \quad \frac{\partial^2 w}{\partial z^2} = 0$$

If the boundaries of the layer are material surfaces, then

$$\begin{aligned} w_n &= \frac{D}{Dt}Z_n + \frac{z - Z_n}{Z_{n-1} - Z_n}\left(\frac{D}{Dt}Z_{n-1} - \frac{D}{Dt}Z_n\right) \\ &= \frac{D}{Dt}Z_n + \frac{z - Z_n}{h_n}\frac{D}{Dt}h_n \end{aligned}$$

with

$$Z_n = \eta - h_1 - h_2 - \ldots - h_n$$

The mass equation becomes

$$\nabla \cdot \mathbf{u} + \frac{1}{h_n}\frac{D}{Dt}h_n = 0$$

or

$$\frac{\partial}{\partial t}h_n + \nabla \cdot (\mathbf{u}_n h_n) = 0 \tag{5.31}$$

The set 5.xx-xx is a discretized version of the inviscid, hydrostaic, Boussinesq model. We can easily add mixing of mementum and traces within a layer; we can also allow a mass flux across interfaces so that

$$w(x, y, Z_n, t) = \frac{D}{Dt}Z_n + w_e$$

but will need a procedure for specifying the entrainment w_e.

In the more complex models of Bleck (19xx) and Hallberg (20xx), some property which is adiabatically conserved and monotonic in depth (call it θ) becomes the vertical coordinate. The equivalent of h_i is $\frac{\partial z}{\partial \theta}$ and the mass and horizontal momentum equations are the same.

For the layered models, the potential vorticity is much simpler: in each layer,

$$q_n = \frac{\zeta + f}{h_n}$$

is conserved by the inviscid dynamics. To see this, we start with the vorticity equation

$$\frac{\partial}{\partial t}\zeta + \nabla \cdot (\mathbf{u}[\zeta + f]) = 0$$

or

$$\frac{\partial}{\partial t} h_n q_n + \nabla \cdot (\mathbf{u} h_n q_n) = 0$$

Using the mass equation 5.xx gives

$$\frac{\partial}{\partial t} q_n + \mathbf{u} \cdot \nabla q_n = 0 \tag{5.32}$$

5.6 — Energetics

The equation for kinetic energy results from dotting the momentum equations with $\overline{\rho}\mathbf{u}$:

$$\frac{\partial}{\partial t} K + \nabla \cdot (\mathbf{u}\overline{\rho}\phi + \mathbf{u}K) = wB + \overline{\rho}\mathbf{u} \cdot Diss \quad , \qquad K = \frac{1}{2}\overline{\rho}|\mathbf{u}|^2$$

The dissipation term should be negative-definite (in addition to a divergence term); it will be if *DIss* takes the standard form $\nu\nabla^2\mathbf{u}$ and $\mu \equiv \overline{\rho}\nu$ is constant. Alternatively, a Crtesian form (as discussed previously) like $\frac{1}{\overline{\rho}}\nabla \cdot \nu\overline{\rho}\nabla\mathbf{u}$ will give energy dissipation of

$$\frac{\partial}{\partial x_i}[\frac{1}{2}\overline{\rho}\nu\frac{\partial u_j u_j}{\partial x_i}] - \overline{\rho}\nu\frac{\partial u_j}{\partial x_i}\frac{\partial u_j}{\partial x_i}$$

so that we get a transport term and one which will dissipate energy.

Kinetic energy can be increased by the uplift of warm fluid $wB > 0$; this energy comes from the potential/ internal energy of the system $P = -\overline{\rho}zB$. The potential energy equation is

$$\frac{\partial}{\partial t} P + \nabla \cdot (\mathbf{u}P) = -wB - \nabla \cdot [z\overline{\rho}\kappa\frac{\partial B}{\partial z}] + \overline{\rho}\kappa\frac{\partial B}{\partial z}$$

when the buoyancy diffuses with the same kind of law as the momentum. The total energy $K + P$ is altered by the divergence of advective fluxes of energy and diffusive fluxes, by dissipation, and by pressure work $-\nabla \cdot \overline{\rho}\mathbf{u}\phi$.

5.7 — Some examples

We now give a few examples with varying scales of motion to illustrate the general procedures of setting up a model and exploring the implications.

5.7.1 — Topographic generation of waves

Flow of stratified fluid over topographic hills will generate waves as the fluid lifts up and creates horizontal buoyancy gradients, which, in turn, generate vorticity. For small scale features $L < U/f$, we expect to find gravity waves, whereas larger scale topography can generate Rossby waves. Tidal flows over banks can create nonlinear wave packets each tidal cycle (cf xx,xx). For a scale small enough that the f-plane approximation applies and water shallow enough that $\rho_a \sim$ const; the Boussinesq equations xx.xx are adequate. We assume something, perhaps tidal forces or mesoscale pressure gradients, is forcing a large-scale depth-independent flow $U(t)$. The interactions with the topography, expressed in the bottom boundary condition

$$w(\mathbf{x}, -H, t) = -[U\hat{\mathbf{x}} + \mathbf{u}(\mathbf{x}, -H, t)] \cdot \nabla H$$

will generate internal waves which can either propagate upwards or decay away vertically.

The linearized problem

$$\begin{aligned} D\mathbf{u} + f\hat{\mathbf{z}} \times \mathbf{u} &= -\nabla\phi + B\hat{\mathbf{z}} \\ \nabla \cdot \mathbf{u} &= 0 \\ DB + wN^2 &= 0 \\ D &\equiv \frac{\partial}{\partial t} + U\frac{\partial}{\partial x} \\ w(\mathbf{x}, -H_0, t) &= -U\frac{\partial}{\partial x}(H - H_0) \\ w(\mathbf{x}, 0, t) &= 0 \end{aligned}$$

can be simplified by using the divergence of the horizontal momentum equations plus the mass equation

$$D\frac{\partial w}{\partial z} + f\zeta = \nabla_h^2 \phi$$

Combining this with the vertical momentum equation and eliminating the pressure gives

$$D\nabla^2 w + f\frac{\partial \zeta}{\partial z} = \nabla_h^2 B$$

with the ∇^2 being the full three-dimensional derivative. Operating on this equation with D and combining with the vorticity equation

$$D\zeta = f\frac{\partial w}{\partial z}$$

(or rather its z-derivative) and ∇_h^2 of the buoyancy equation gives an expression for the vertical velocity

$$D^2\nabla^2 w + f^2\frac{\partial^2}{\partial z^2}w + N^2\nabla_h^2 w = 0$$

to be solved with the boundary conditions above. Fourier-analyzing the topographic variation

$$H - H_0 = \int d\mathbf{k} \hat{H}(\mathbf{k}) \exp(\imath \mathbf{k} \cdot \mathbf{x})$$

and the vertical velocity leads to

$$\left(\frac{\partial}{\partial t} + \imath k U \right)^2 \left(\frac{\partial^2}{\partial z^2} - |\mathbf{k}|^2 \right) \hat{w} + f^2 \frac{\partial^2}{\partial z^2} \hat{w} - N^2 |\mathbf{k}|^2 \hat{w} = 0 \quad , \quad \hat{w}(0) = 0 \quad , \quad \hat{w}(-H_0) = -\imath k U \hat{H}$$

In the case of steady flow and constant N, solutions are

$$\hat{w} = \imath k U \hat{H} \frac{\sin(mz)}{\sin(mH_0)}$$

with

$$m^2 = |\mathbf{k}|^2 \frac{N^2 - k^2 U^2}{k^2 U^2 - f^2}$$

If the effective frequency kU is between f and N, m will be real, and the waves will vary sinusoidally; otherwise, the $\sin mz$ functions are replaced by $\sinh |m| z$, resulting in waves which decay exponentially in the vertical. Figure 5.xx shows examples of the vertical velocity patterns.

The sinusoidal case has some peculiarities because of the sea surface. Essentially, the topography creates an upward propagating wave (in the sense of group velocity or energy) which reflects off the top boundary and eventually sets up a standing wave form (figure 5.xx). In reality, waves in the deep ocean may not survive the round-trip: they may become nonlinear enough to break or be affected by shear in the large-scale flow such that the rate of propagation drops to zero. Thus, we should discuss the problem in which the wave is assumed to have upward propagation of energy and the reflected wave is not present. We replace the top boundary condition by a "radiation condition" somewhere above the topography. This is straightforward for the linear problem, but more difficult for the nonlinear one; instead, a "sponge layer" is commonly used to absorb the upward wave with minimal reflection. We shall discuss both.

From the energy equation, upward vertical flux corresponds to $\overline{\rho} w \phi > 0$; for the unbounded system with

$$w = \Re[\imath k U \hat{H} \exp(\imath k x + \imath m z)] \equiv \Re[\hat{w} \exp(\imath k x + \imath m z)]$$

(taking $z = 0$ as the mean ocean bottom), we find

$$\phi = \Re[m \frac{k^2 U^2 - f^2}{k^3 U} \hat{w} \exp(\imath k x + \imath m z)]$$

when the solutions are propagating, rather than exponentially decaying, $k^2 U^2 > f^2$ so that solutions with upward energy flux will have $m > 0$. Figure 5.xx shows this orientation. In a frame moving with the zonal flow, these appear to have phase propagation which

is downwards and westwards. As shown above (e.g., figure 5,xx), the group velocity is upwards, carrying the energy upwards.

The sponge-layer approach is equally straightforward: we add a term $-r(z)\mathbf{u}$ and $-r(z)B$ to the momentum and buoyancy equations respectively. (If the topography is isolated, waves will also carry energy in the x direction, so that we would impose $r = r(x, z)$.) For the 2-D topography, the vorticity, along-topography momentum, and buoyancy equations

$$\begin{aligned} Dq &= f\frac{\partial v}{\partial z} - \frac{\partial B}{\partial x} - \nabla \cdot r\nabla\psi \\ Dv &= -rv - f\frac{\partial \psi}{\partial z} \\ DB &= -rB + N^2\frac{\partial \psi}{\partial x} \\ q &= \nabla^2\psi \end{aligned}$$

can be stepped forward to give the steady solution shown in figure 5.xx. The steady-state waves look like those found in the undamped problem before the reflection from the top; likewise, they have the tilts predicted from the radiation condition.

5.7.2 — Flow around islands and Taylor columns

Let us consider zonal flow against an island or a seamount. We will use the QG form of a two-layer model (c.f., Pedlosky, 19xx). In each layer, we expand the variable part of the potential vorticity

$$Q_n = H_n q_n - f_0 = \frac{1}{1+\delta_n}(\zeta_n + \beta y - f_0\delta_n)$$

where the β-plane approximation has been used, and $\delta_n = (h_n - H_n)/H_n$ is the thickness anomaly divided by the mean layer thickness H_n. For the QG version, we just drop the δ_n in the denominator and replace the velocities and pressure by the geostrophic streamfunction

$$\mathbf{u}_n = \hat{\mathbf{z}} \times \nabla\psi_n \quad , \quad \phi_n = f_0\psi_n$$

so that

$$f_0(\psi_1 - \psi_2) = g' H_1\delta_1 \quad , \quad g' = \frac{\rho_1 - \rho_2}{\rho_2}g$$

Our equations become

$$\frac{\partial}{\partial t}Q_n + \mathbf{u}_n \cdot \nabla Q_n = 0 \tag{5.33}$$

with

$$\mathbf{u}_n = \hat{\mathbf{z}} \times \nabla\psi_n$$

and

$$\begin{aligned} Q_1 &= \nabla^2\psi_1 + \frac{f_0^2}{g' H_1}(\psi_2 - \psi_1) + \beta y \equiv (\nabla^2 - F_1)\psi_1 + F_1\psi_2 + \beta y \\ Q_2 &= \nabla^2\psi_2 + \frac{f_0^2}{g' H_2}(\psi_1 - \psi_2) + \beta y + f_0\frac{H_b}{H_2} \equiv (\nabla^2 - F_2)\psi_2 + F_2\psi_1 + \beta y + f_0\frac{H_b}{H_2} \end{aligned}$$

with $F_j = f_0^2/g'H_j$.

We begin with a 500 m topographic hill (with width of 25 km) in the bottom layer and turn on a zonal flow U_n. The flow pushes fluid off of the hill and replaces it with fluid from upstream. The former experiences stretching, developing cyclonic vorticity, while the latter creates an anticyclone on top of the hill. The resulting dipole would propagate southward; however, the anticyclone remains pinned over the hill, and the cyclone rotates around to the south. If the flow is strong enough, this eddy is carried off to the west (Huppert and Bryan, 19xx; figure 5.xx). For weak flows, the cyclone wraps around and we end up with a pattern of waves to the east of the hill (5.xx).

5.7.3 — Propagation of eddies

5.7.4 — Simple models of gyres

5.8 — Instabilities of fluid flow

We have seen that nonlinearities in the biological equations can cause instabilities in the sense that two states which are initially very close to each other will, in time, become very different. In the most common cases, one state is an equilibrium solution; when perturbations from this state grow, it is classified as unstable. But unsteady solutions can also be stable or unstable depending on whether neighboring trajectories diverge (usually at an exponential rate). Instabilities are ubiquitous in fluid systems. Smooth, laminar motions are rare, and, instead, we see irregular flows filled with eddies and turbulence. For large-scale atmospheric weather systems or their analogues, the oceanic mesoscale, limits on predictability are linked to the instability of these time-varying solutions to the relevant equations of motion.

In principle, the theory of fluid instabilities simply generalizes the one presented for $b_i(t)$ in chapter xx to a very large system for discretized models – the variables become the fields defined at each grid point. Consider the barotropic vorticity equation for which the flow is determined by a single scalar field $q(\mathbf{x}, t)$. On a coarse 32×32 grid, the state of the system is defined by the 1024 values of q, already large enough to make evaluation of matrix eigenvalues questionable. For this or larger systems, we may still be able to find growth rates for the dominant mode by linearizing and time-stepping, but, in general, we will want to study the continuum system.

To develop the theory, we shall work with the barotropic vorticity equation

$$\frac{\partial}{\partial t} q + \mathbf{u} \cdot \nabla q = 0 \quad , \quad \mathbf{u} = \hat{\mathbf{z}} \times \nabla \psi \quad , \quad q = \nabla^2 \psi + \beta y$$

We assume we know a solution, called the "basic state," $\overline{q}(\mathbf{x}, t)$; in classical problems, this is a steady solution $\overline{q}(y)$ but other cases are of interest as well. If we consider a solution which is initially nearby

$$q(\mathbf{x}, t) = \overline{q}(\mathbf{x}, t) + q'(\mathbf{x}, t)$$

with $||q'(\mathbf{x}, 0)||$ small (in a sense yet to be defined), then the flow will be stable if $||q'(\mathbf{x}, t)||$ remains small and unstable if it does not.

A flow is stable in the sense of Lyapunov if all perturbations started in some range $0 < ||q'(\mathbf{x},0)|| < \delta$ remain bounded $||q'(\mathbf{x},t)|| < \epsilon$; formally, we need to ensure that given any choice of ϵ, we can indeed find a nonzero δ such that this holds.[†] To measure perturbation amplitudes, we can, for example, compute the eddy energy

$$||q'|| = \frac{1}{2}\iint u'^2 + v'^2 = -\frac{1}{2}\iint \psi' q'$$

(given suitable boundary conditions). At first sight, we might think this is constant, since, for inviscid problems, energy is conserved, and the basic state energy from $\frac{1}{2}\overline{\mathbf{u}}^2$ is constant, but that is not the case. For unstable flows, the $\frac{1}{2}\mathbf{u}'^2$ perturbation energy can grow because the $\overline{\mathbf{u}} \cdot \mathbf{u}'$ term becomes more and more negative. We often deal with only the first order in perturbation amplitude; by the balance above, $\iint \overline{\mathbf{u}} \cdot \mathbf{u}'$ must be second order, so that we do not calculate it explicitly.

For unstable systems, twin experiments in which the full equations are solved for the basic state and the perturbed system can show the divergence and growth of perturbation energy. Stability can be much harder to demonstrate numerically; sometimes analytical methods can be useful (c.f. Shepherd, 19xx) but often we are left with a result (e.g, that random perturbations do not grow) suggesting, but not proving, stability.

Most of the time, however, the question is approached using the linearized system obatined by subtracting the basic state dynamical equation from the full equation

$$\frac{\partial}{\partial t}q' + \overline{\mathbf{u}} \cdot \nabla q' + \mathbf{u}' \cdot \nabla \overline{q} + \mathbf{u}' \cdot \nabla q' = 0 \tag{5.34}$$

and then dropping the last term for analysis of the phase when the perturbations are very small but may be growing

$$\frac{\partial}{\partial t}q' + \overline{\mathbf{u}} \cdot \nabla q' + \mathbf{u}' \cdot \nabla \overline{q} \simeq 0 \tag{5.35}$$

If $\overline{q}$ (and therefore $\overline{\mathbf{u}}$) is steady, the linearized problem 5.xx will have exponential normal mode solutions

$$q' = \hat{q}(\mathbf{x}) \exp(\sigma t)$$

and the flow will be unstable if any σ's have a positive real part.

If we have discretized the problem in space, so that

$$\frac{\partial}{\partial t}q'(\mathbf{x}_i) = M_{ij} q'(\mathbf{x}_j)$$

the σ values form a discrete set – the eigenvalues of $\mathbf{M}$. (Sometimes the eigenvalues have a non-zero multiplicity; this corresponds to solutions depending on powers of t as well as the exponential.) Sometimes the eigenvalues are ill-defined, especially for large matrices, being very sensitive to resolution or downstream wavenumber. In that case, we may be

[†] Stable if for all $\epsilon > 0$ there exists a $\delta > 0$ such that for all initial states with $||q'(\mathbf{x},0)|| < \delta$, $||q'(\mathbf{x},t)|| < \epsilon$.

able to examine instabilities by integrating 5.xx, starting with random initial conditions, plotting $\ln ||q'||$, and looking for a time when it grows exponentially. Unlike the matrix eigenvalue approach, this method only gives te σ and the structure of the most rapidly growing mode, but that is often sufficient.

The truly continuous problem is more complex: there will be a few eigenmodes (non-trivial solutions to

$$\overline{\mathbf{u}} \cdot \nabla q' + \mathbf{u}' \cdot \nabla \overline{q} = -\sigma q'$$

which satify the appropriate boundary conditions), but these do not form a complete set (c.f., Case,19xx). For the remaining discussion, we consider the most common problem, the growth of perturbations on a zonal flow $\overline{\mathbf{u}} = U(y,z)\hat{\mathbf{x}}$, $\overline{q} = Q(y,z)$. The disturbances can be fourier-analyzed in x; normal modes take the form

$$q' = \hat{q}(y,z)\exp(\imath k[x-ct])$$

and are unstable if the imaginary part of c is positive. The modes are found by solving the Rayleigh equation

$$Uq' + \left(\beta - \frac{\partial^2 U}{\partial y^2}\right)\psi' = cq' \quad , \qquad \left(\frac{\partial^2}{\partial y^2} - k^2\right)\psi' = q' \tag{5.36}$$

If we think of ψ' as $\left(\frac{\partial^2}{\partial y^2} - k^2\right)^{-1} q'$, we can see the relationship to a matrix eigenvalue problem when this operator is discretized. We shall show some examples below.

Case (19xx) and others have examined the initial value problem

$$\frac{\partial}{\partial t}q' + \imath k U q' + \imath k \frac{\partial Q}{\partial y}\left(\frac{\partial^2}{\partial y^2} - k^2\right)^{-1} q' = 0$$

and shown that the normal modes must be augmented by a set of "singular modes" or "continuum modes" for which $\frac{\partial \psi}{\partial y}$ has a discontinuity at $y = y_d$. The net effect of these (integrated over y_d) results in an algebraic decay at large times. Yet they still may be important; Farrell (19xx, 19xx) argues that many atmospheric phenomena behave more like the transient response when many differenct modes are interfering or reinforcing each other rather than the long-time exponential growth of a single normal mode. No doubt, the same applies to the ocean.

Finally, we note that a localized perturbation may move downstream faster than it grows. At a single monitoring point, the disturbance first increases and then decays; for a point further downstream, the amplitude peaks at a larger value. For strong currents like the Gulf Stream, Thacker (19xx) and Ni (19xx) have shown that this form of downstream growth (known in a somewhat unfortunate terminology as "convective" instability) appears most appropriate. Individual peaks can amplify several times faster than the most rapidly growing periodic wave (Ni, 19xx). Correspondingly, we may expect to find stronger pulses of upwelling.

Other instabilities may be "absolute," rather than "convective": the propagation is slow enough so that the decay as the pulse moves by is overcome by the unstable growth. At each point, then, the disturbance continues to amplify in time.

Such considerations seem abstruse, but they can significantly alter the way we interpret measurements to infer growth rates. Upwelling and transport can be quite different for localized, rapidly growing disturbances, so that process models using linear instability theory to estimate biological impacts (e.g., along the Florida current system; c.f. Hoffmann, 19xx) need to address a broader class of motions. Most importantly, we must also not lose sight of the fact that disturbances do not remain linear; by the time they are observed, the differences between the currents and those in some underlying basic state will be the same order as the flows themselves. Linear theory can be a useful interpretive tool, but misses significant aspects of the dynamics: the process that sets the amplitudes of the waves, the alterations in structure which can alter the transport and upwelling, and whether the waves equilibrate, oscillate, or become chaotic. The analytical parts of the following subsections, then, must be regarded as explicating the dynamics rather than providing models that can be used for process studies, unlike the numerical parts which will address the nonlinear effects.

5.8.1 — Convection

As the sea-surface cools at night or over the winter, the water may become denser than the underlying fluid. If the isopycnals are perturbed from level, horizontal buoyancy gradients are produced which, in turn, begin to produce vorticity. As sketched in figure 5.xx, the flows will further lift the light fluid and draw the heavier fluid down; the layer tries to overturn (refer to equation 5.xx). This process can be retarded by viscosity, but also by conduction which reduces the density contrast.

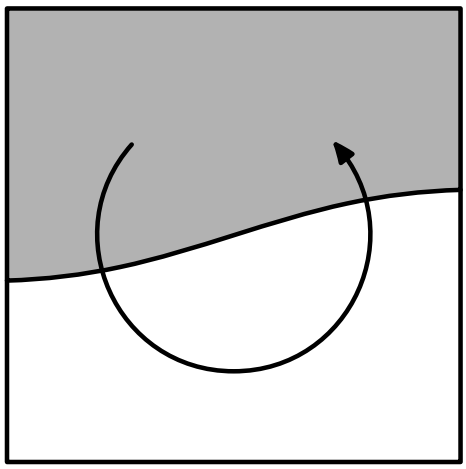

Figure 5.6: Sketch in x-z plane of perturbed heavy fluid over light fluid. The buoyancy gradient $\frac{\partial}{\partial x}B > 0$, generating negative vorticity around the y axis and producing flows in the sense shown, enhancing the perturbation.

Although 3D effects appear soon after the instability, the 2D problem can describe both the instability and some of the effects of nonlinearity. It can be phrased in terms of the vorticity $q \equiv \zeta_y$ and buoyancy

$$\begin{aligned}
\frac{\partial}{\partial t} q + \mathbf{u} \cdot \nabla q &= f \frac{\partial v}{\partial z} - \frac{\partial B}{\partial x} + \nu \nabla^2 q \\
\frac{\partial}{\partial t} v + \mathbf{u} \cdot \nabla v &= -f u + \nu \nabla^2 v \\
\frac{\partial}{\partial t} B + \mathbf{u} \cdot \nabla B &= -\nabla \cdot (Q - \kappa \nabla B) \\
q = \nabla^2 \psi \qquad & u = \frac{\partial}{\partial z} \psi \ , \quad w = -\frac{\partial}{\partial x} \psi
\end{aligned} \tag{5.37}$$

The standard problem ignores the buoyancy flux associated with the radiation Q and imposes the temperature (buoyancy) at upper and lower boundaries. We shall instead consider penetrative solar radiation, assumed to be absorbed at a constant rate, so that

$$Q = -Q_s \exp(z/h_\ell)$$

where Q_s is the surface insolation (converted to a buoyancy flux so having units L^2/T^3) and h_ℓ is the decay scale (order $20m$). Of course, the insolation should be time-dependent (which significantly complicates the stability problem) and have multiple decay scales for the different wavelengths (which is a relatively simple change). Heat is lost at the sea-surface to compensate the solar input and a small amount diffusing down into the deeper stratification

$$\kappa \frac{\partial B}{\partial z}\Big|_{z=0} = \kappa N^2 - Q_s$$

The diffusive solution is just

$$\kappa \frac{\partial B}{\partial z} = \kappa N^2 - Q_s \exp(z/h_\ell) \quad \Rightarrow \quad B = N^2 z - \frac{Q_s h_\ell}{\kappa} \exp(z/h_\ell)$$

The nondimensional version of this formula

$$\frac{B}{N^2 h_\ell} = \frac{z}{h_\ell} - \frac{Q_s}{\kappa N^2} \exp\left(\frac{z}{h_\ell}\right) \tag{5.38}$$

shows that the profiles depend on a single parameter $\Delta_q \equiv Q_s/\kappa N^2$; when this is larger than one, we have heavier (low buoyancy) fluid overlying lighter fluid.

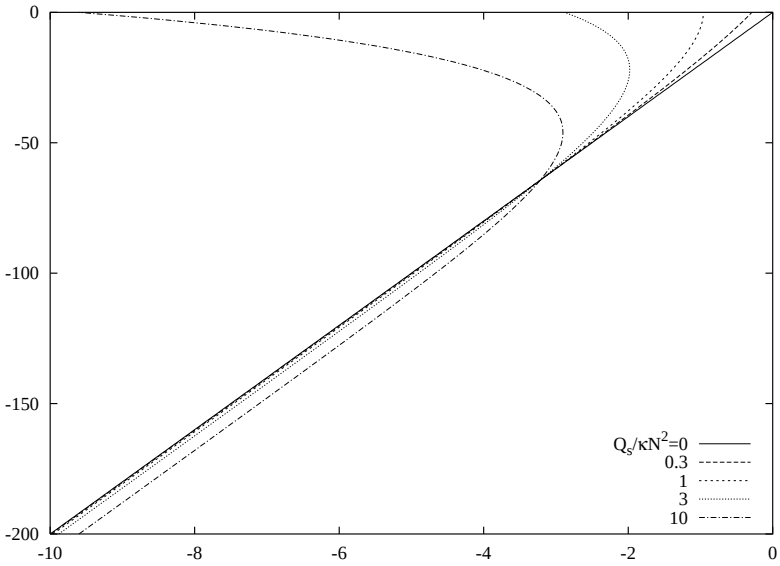

Figure 5.7: Profiles of B for various solar forcing strengths.

Using a basic state profile $\overline{B}(z)$ satisfying the diffusive–heating balance 5.xx, we have the stability problem

$$(\frac{\partial}{\partial t} - \nu\nabla^2)q' - f\frac{\partial v'}{\partial z} + \frac{\partial B'}{\partial x} = 0$$
$$(\frac{\partial}{\partial t} - \nu\nabla^2)v' + f\frac{\partial \psi'}{\partial z} = 0$$
$$(\frac{\partial}{\partial t} - \kappa\nabla^2)B' - \frac{\partial \psi'}{\partial x}\frac{\partial \overline{B}}{\partial z} = 0$$

We have 6 dimensional parameters and 2 units (length and time), so that the system is defined by 4 nondimensional parameters; conventionally these would be the Rayleigh, Taylor, Prandtl, and (because of the deep N) a stratification number

$$Ra = (\Delta_q - 1)\frac{N^2 h_\ell^4}{\nu\kappa^2} \quad , \quad Ta = \frac{f^2 h_\ell^4}{\nu^2} \quad , \quad Pr = \frac{\nu}{\kappa} \quad , \quad S = \frac{N^2}{f^2}$$

The Rayleigh number is defined here in terms of the $|\frac{\partial \overline{B}}{\partial z}|$ value at the surface , $Q_s/\kappa - N^2 = (\Delta_q - 1)N^2$. The boundary conditions at the surface are

$$\frac{\partial B'}{\partial z} = \psi' = q' = \frac{\partial v'}{\partial z} = 0$$

corresponding to a strict specification of the heaat flux, vanishing shear stress and vertical velocity.

Numerical solutions indicate that the critical Rayleigh number (given molecular parameters for ν, κ) is order 10^{12}; however, this is a misleading number. The critical value of Δ_q appears to be near 1.004, so that the depth range over which the density gradient is reversed is $h_\ell \ln \Delta_q$, is only about about 8 cm. (Therefore, the resolution for the numerical

stability calculation is about 5 mm.) If we use this instead of h_l in the Rayleigh number, we find a value order 220. For reference, the critical Ra with a constant gradient and fixed flux at the top and bottom is $\pi^4 = 97.4$; not surprisingly, our number is higher since the gradient decreases to zero over these top 8 cm so that the average gradient is about half the peak value. In addition, the motions do extend into the stably stratified layer, requiring additional kinetic energy to be extracted from the sinking of heavier fluid and the rising of lighter water.

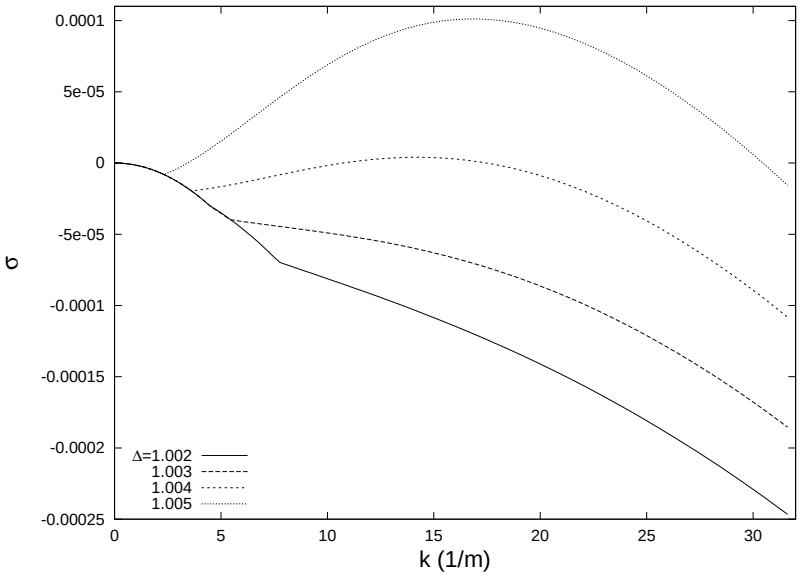

Figure 5.8: Growth rates as a function of horizontal wavenumber for various solar forcing strengths.

Given that the critical solar flux is very close to that carried by diffusion in the stratified layer, it is not surprising that the dimensional surface heat flux $H_s = Q_s \rho c_p / \alpha g$ works out to be about 0.15 $watts/m^2$. Typical fluxes are three orders of magnitude higher, so that we can expect to be far into the supercritical range. For a heat flux of 100 W/m^2, $\Delta_q \sim 670$, and the stratification in negative over the top 130 m. Covering both a large enough (perhaps a kilometer in depth) domain is out of the question if we wish to resolve the dissipation scales.

As the instability develops, the upper layer becomes fairly well-mixed; to see this, we have simulated the 2D equations with the 100 W/m^2 heat flux. To keep the calculation manageable, we have used a 2 m spatial resolution and increased the effective viscosity to 10^{-3} m^2/s, keeping the Prandtl number at 8 ($\Delta_q = 179$). We used a 256×512 m domain and integrated for a month (in a shallower system, the internal waves generated by the plumes and reflecting off the artifical bottom boundary have a noticeable effect). Figure 5.xx shows the buoyancy (which can be thought of as temperature) and vorticity at various times. Plumes form, detaching from the cooled surface and, descending, generate dipolar vortices which increase the downward speed. Note the internal waves, generated as the plume hits the stratified base of the well-mixed layer. in the deep water in the 10 day snapshot. These mix and form a fairly homogeneous region – a mixed layer – which deepens over several weeks (figure 5.xx).

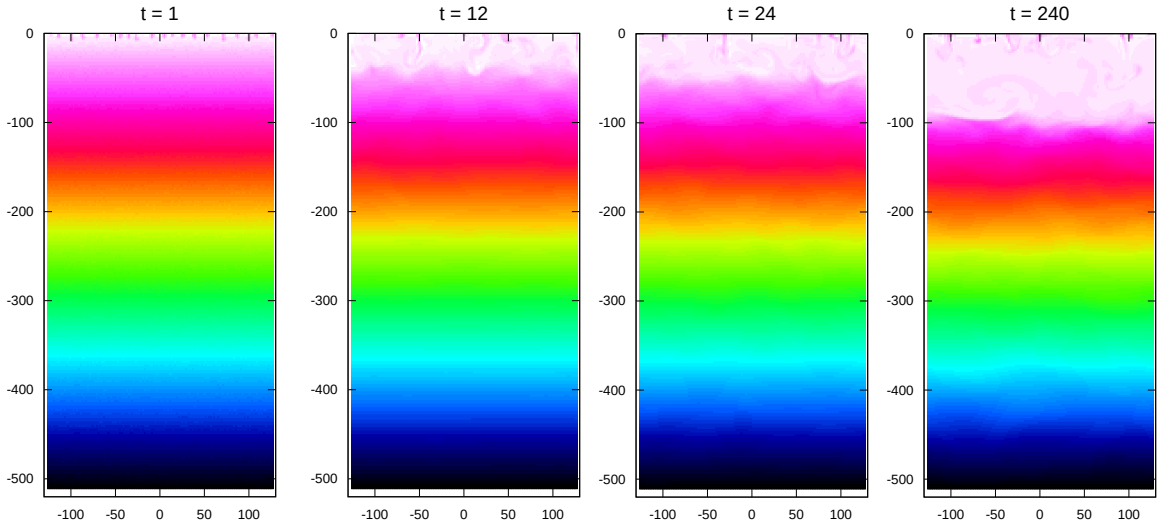

Figure 5.9a: Buoyancy fields at $t = 1$, 12, 24, and 240 hr after the heating and cooling commences.

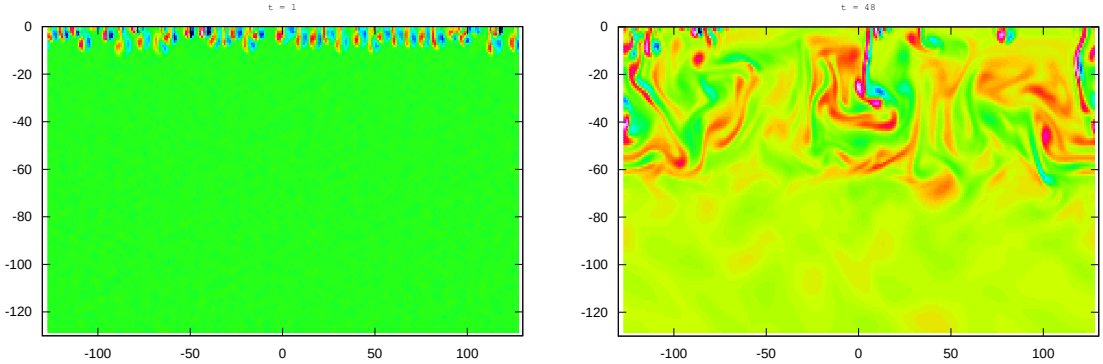

Figure 5.9b: Vorticity field in the upper part of the regime for a run with double resolution. Note the dipole structures associated with the down-welling plumes.

In this detailed model of a convectively-mixed layer, the deepening effectively halts when the buoyancy flux from the convective plumes can balance the heat fluxes. From the terms in the horizontally averaged buoyancy equation

$$\frac{\partial}{\partial t}\overline{B} = -\frac{\partial}{\partial z}\left[\overline{w'B'} - \kappa\frac{\partial}{\partial z}\overline{B} + Q\right]$$

(figure 5.xx), we can see that the vertical flux by the convection indeed nearly balances the heating throughout the mixed layer, Near the surface, the eddy flux, $\overline{w'B'}$, vanishes so that the solar heating is balanced by diffusion; correspondingly, the mean buoyancy profile (5.xx) does show a region of negative gradient within the top few meters. The base of

the mixed layer is somewhat more complex. As the heat flux picture shows, the vertical momenum in the plume is large enough that it passes the point of neutral buoyancy and begins to push warmer water down into colder regions ($\overline{w'B'} < 0$).

In addition to winter-time formation of water masses such as the 18° water in the North Atlantic and the production of Antarctic bottom water, convection occurs on continental shelves, the Arctic and the Mediterranean. In addition, the hot outflow from deep ocean vent systems produces strong convective plumes.

5.8.2 — Shear

Convection can be understood simply as fluid with negative buoyancy tending to fall while buoyant fluid rises. Shear instability is less intuitive; it involves waves which can reinforce each other to produce amplification. The waves are vorticity waves (c.f. figures 5.xx and 5.xx), but the vorticity gradient here is the one associated with the basic state flow. For example, let us examine a shear layer

$$U = U_0 \tanh(y/L)$$

On the β-plane, the potential vorticity and its gradient are

$$Q = \beta y - \frac{\partial U}{\partial y} \quad , \quad \frac{\partial Q}{\partial y} = \beta - \frac{\partial^2 U}{\partial y^2} = \beta + \frac{2U_0}{L^2} \operatorname{sech}^2(y/L) \tanh(y/L)$$

(figure 5.xx). For large enough shear, $|U_0| > \frac{3\sqrt{3}}{4}\beta L^2$, the gradient of potential vorticity is negative in the southern part of the region (taking $U_0 > 0$). Outward perturbations of lines of fluid particles will generate negative anomalies when the lines are centered in regions with opposite PV gradients (figure 5.xx). The anticyclonic circulations associated with these anomalies tend to further perturb the opposite line, giving rise to growth. The wave-like aspect arises because the anomalies also tend to propagate (westward or eastward for $\frac{\partial Q}{\partial y}$ positive or negative) and to be advected by the shear flow $U(y)$. If the propagation and advection speeds are suitably matched, the anomalies will remain in the same phase-shifted orientation with respect to each other and growth continues. Figure 5.xx shows the growth rates from solving the discretized version of 5.xx; the nonlinear growth and roll-up of the shear layer is very similar to that shown in the next section (figure 5.xx). As time goes on the layer widens by successive mergers of different neighboring vortices; c.f. xx, 19xx).

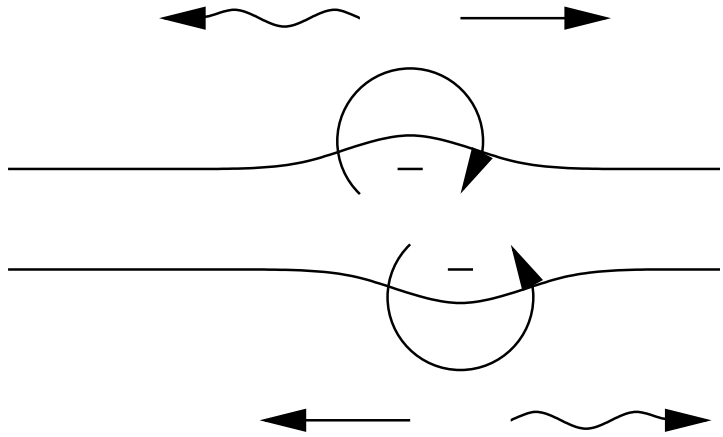

Figure 5.10: Perturbations on the shear flow which can enhance each other. The negative anomalies in vorticity are associated with the flows shown. The propagation direction is indicated by the wavy arrow, and the advection by the straight one.

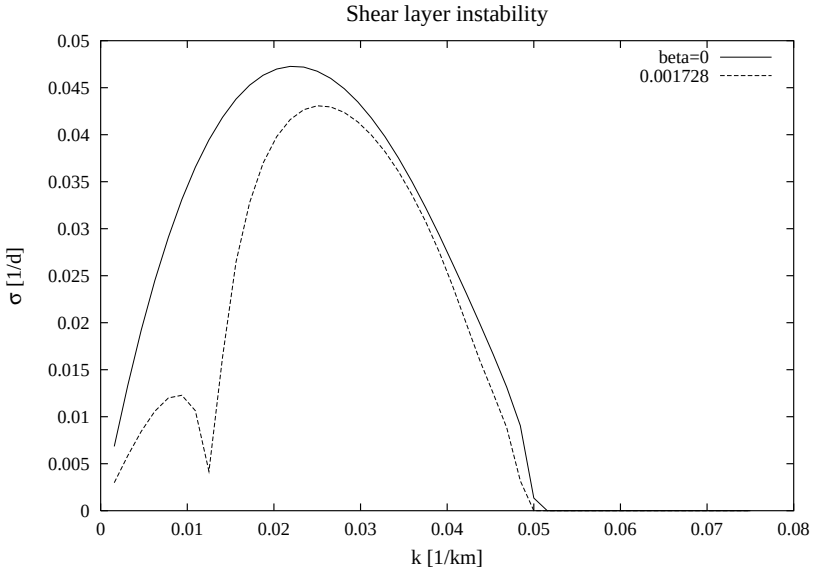

Figure 5.11: Growth rate for perturbations on the tanh shear layer with $U_0 = 5\ km/d$, $L = 20\ km$. The beta values are in $km^{-1}d^{-1}$.

Examining the energetics of the perturbations can be helpful in visualizing the flow structures. If we dot the linearized perturbation momentum equations

$$\frac{\partial}{\partial t}\mathbf{u}' + Q\hat{\mathbf{z}} \times \mathbf{u}' + q'\hat{\mathbf{z}} \times U\hat{\mathbf{x}} = -\nabla(\phi' + Uu')$$

with $\mathbf{u}'$, we have

$$\frac{\partial}{\partial t}\frac{1}{2}|\mathbf{u}'|^2 + Uv'q' + \nabla\cdot(\mathbf{u}'\phi' + Uu'\mathbf{u}') = 0$$

The x-averaged equation

$$\frac{\partial}{\partial t}\frac{1}{2}\overline{|\mathbf{u}'|^2} - U\overline{v'\frac{\partial u'}{\partial y}} + \frac{\partial}{\partial y}U\overline{u'v'} + \frac{\partial}{\partial y}\overline{v'\phi'} = 0$$

yields

$$\frac{\partial}{\partial t}\frac{1}{2}\overline{|\mathbf{u}'|^2} + \overline{u'v'}\frac{\partial U}{\partial y} + \frac{\partial}{\partial y}\overline{v'\phi'} = 0$$

when we use the mass conservation equation and $\overline{g'\frac{\partial}{\partial x}g'} = 0$ for any g. For the perturbation energy to grow, the transport of eastward momentum must be on averagre southward in regions of positive shear and northward in regions of negative shear. This down-gradient flux reduces the contrast in the zonally averaged flow, extracting kinetic energy which then fuels the growth.

The most famous result for general shear flows is Rayleigh's theorem (Rayleigh, 18xx, Charney and Stern, 19xx) which states that if $\frac{\partial}{\partial y}Q$ is uniform in sign within the domain, the flow will be stable. Therefore, a necessary condition for instability is that $\frac{\partial}{\partial y}Q$ must change sign. For a simple derivation, we examine the enstrophy balance

$$\frac{\partial}{\partial t}\frac{1}{2}q'^2 = -\overline{v'q'}\frac{\partial Q}{\partial y}$$

In order for the enstrophy of the perturbation to grow, the flux of PV $\overline{v'q'}$ must, on average, be down gradient (opposite sign to $\frac{\partial Q}{\partial y}$). If we look at the displacements of the PV contours

$$Q(y+\eta') + q'(x, y+eta', t) = Q(y) \quad \Rightarrow \quad q'(x,y,t) \simeq -\eta'\frac{\partial Q}{\partial y}$$

then

$$\frac{\partial}{\partial t}\eta' + U\frac{\partial}{\partial x}\eta' = v'$$

and

$$\overline{v'q'} = -\frac{\partial}{\partial t}\frac{1}{2}\overline{\eta'^2}\frac{\partial Q}{\partial y}$$

Thus the flux can be written as an eddy diffusivity acting on the mean gradient (but not one which is spatially uniform or independent of the background state itself since the growthrate is a functional of Q). If the perturbation is growing, the eddy diffusivity will be positive, the flux is down-gradient as required for growth. But, we also note that the integrated flux

$$\int dy\overline{v'q'} = -\int dy\frac{\partial}{\partial y}\overline{v'u'} = 0$$

Thus, we have

$$\int \left[\frac{\partial}{\partial t} \frac{1}{2} \overline{\eta'^2} \right] \frac{\partial Q}{\partial y} = 0$$

which, since the term in brackets is positive definite for a growing mode, implies that $\frac{\partial Q}{\partial y}$ must be positive for some y and negative for others.

Shear instability can occur on many different scales in the ocean. In the cm to m range, turbulence in the bottom boundary layer and in flows around obstacles such as pilings (or, for that matter, fish) arises when the sheared flow breaks up. In the 10's to 100's of km range, we can think of unsteady island wakes and boundary currents as manifesting some form of shear instability (though baroclinic processes, discussed below, may also enter).

5.8.3 — Kelvin-Helmholtz

Shear instability can occur in the same way when we have vertical shear of the horizontal velocity; however, stratification alters the dynamics because the vertical velocities now have to work against the potential energy associated with the stratification. The latter is responsible for the restoring force for internal waves, so we may expect the instability will require more shear. If we multiply the linearized horizontal vorticity equation

$$\frac{\partial}{\partial t} q' + U \frac{\partial}{\partial x} q' - \frac{\partial^2 U}{\partial z^2} \frac{\partial}{\partial x} \psi' = - \frac{\partial}{\partial x} B'$$

by $-\psi'$ and average, gives a kinetic energy equation

$$\frac{\partial}{\partial t} \frac{1}{2} \overline{|\nabla \psi'|^2} - \frac{\partial U}{\partial z} \overline{\frac{\partial \psi'}{\partial x} \frac{\partial \psi'}{\partial z}} - \frac{\partial}{\partial z} [\overline{\psi' \frac{\partial^2 \psi'}{\partial t \partial z}} + U \overline{\psi' \frac{\partial^2 \psi'}{\partial x \partial z}}] = \overline{\psi' \frac{\partial B'}{\partial x}}$$

or

$$\frac{\partial}{\partial t} K' + \overline{u'w'} \frac{\partial U}{\partial z} = \overline{w'B'} - \frac{\partial}{\partial z} flux$$

($K' = \frac{1}{2} \overline{|\mathbf{u}'|^2}$) indicating growth can occur by extracting kinetic energy from the shear or potential energy. But the available potential energy equation, from B'/N^2 times the buoyancy equation,

$$\frac{\partial}{\partial t} P' + \overline{w'B'} = 0$$

($P' = B'^2/2N^2$) shows that a growing perturbation will have $\overline{w'B'}$ negative and must, therefore, have $\overline{u'w'} \frac{\partial U}{\partial z}$ strongly negative. If we estimate $\sigma \mathbf{u}' \sim w' \frac{\partial U}{\partial z}$ and $\sigma b' \sim w' N^2$, the instability will require

$$\frac{w'^2}{\sigma} \left(\frac{\partial U}{\partial z} \right)^2 > \frac{w'^2}{\sigma} N^2$$

so that the Richardson number $N^2/(\frac{\partial}{\partial z} U)^2$ must be less than 1. Arbarbanel, *et al.*(1984) prove that flows with $Ri > 1$ will be nonlinearly stable. In contrast, detailed analyses by Miles (1961) and Howard (1961) show that linear instability can only occur if the Richardson number is smaller that 0.25 somewhere in the flow.

Two-D numerical simulations for $U = U_0 \tanh(z/\ell)$, $B = B_0 \tanh(z/\ell)$ shows no significant growth for $Ri > 0.25$; below that, the waves amplify and roll up into "cats-eyes" (figure 5.xx); subsequently, the vortices merge and form a much broadened shear layer which is now subcritical. We can see secondary instabilities occuring in some cases. Woods (1973) has some beautiful pictures of this phenomenon in the ocean.

These simulations are for $Ri = 0.1$; the case with $Ri = 0.15$ evolve similarly but more slowly. For $Ri = 0.2$, closer to the stability boundary, the waves show up as striations in the q field, but are less obvious in the buoyancy field unless we plot the deviations from the x averaged B. Finally, we note that 3D instabilities of the rolls set in shortly after they form, so that the subsequent evolution will be much more turbulent than indicated by the figures here (c.f., xx, 19xx).

Kelvin-Helmholtz instability acts at the base of the mixed layer (Pollard, *et al.*, 19xx, Price, *et al.*, 19xx) and is probably a major mechanism for entraining deeper fluid into the layer when it is not convectively active. In the atmosphere, internal gravity waves commonly break when the local Richardson number becomes small enough; in the ocean, we anticipate that the same will occur, leading to local generation of turbulence and dissipation.

5.8.4 — Baroclinic

When we consider vertical shear extending over a substantial fraction of the depth, such as the Sverdrup flow in the ocean's interior, the Richardson number will generally be large. But, as Eady (1949) and Charney (1947) showed, the flow can still be unstable because of the effects of rotation. In essence, the thermal wind equation implies that the isopycnals must tilt so that some heavy fluid is higher than average and some light fluid is lower. Therefore, we have available potential energy that can be released if we are able to level the isopycnals. (In terms of the equations above $\overline{B}^2/N^2 > 0$ where $\overline{B}$ is the deviation from the stratified profile $\int^z dz' N^2(z')$ associated with the basic state flow $f\frac{\partial}{\partial z}U = -\frac{\partial}{\partial y}\overline{B}$.)

Perhaps the simplest model for baroclinic instability is that of Phillips (19xx), using the QG two-layer system (5.xx). Oceanographers have usually followed the meteorologists in studing zonal basic state, but we shall take a more general case (c.f. McWilliams and Robinson, 19xx, Arbic and Flierl, 19xx). If the upper layer basic state flow is $\Psi_1 = -U_1 y + V_1 x$, then a lower layer flow $\Psi_2 = -(\beta g' H_1/f_0^2 - \delta U_1)y - \delta V_1 x$ will satisfy the inviscid dynamics $\mathbf{u}_n \cdot \nabla Q_n = 0$. The potential vorticity gradients,

$$\frac{\partial}{\partial x}Q_1 = -\frac{V_1}{R_d^2} \quad , \quad \frac{\partial}{\partial x}Q_2 = \frac{H_1}{H_2}\frac{V_1}{R_d^2}$$

and

$$\frac{\partial}{\partial y}Q_1 = \frac{U_1}{R_d^2} \quad , \quad \frac{\partial}{\partial y}Q_2 = \beta\frac{H_1+H_2}{H_2} - \frac{H_1}{H_2}\frac{U_1}{R_d^2}$$

will change sign in the vertical if $V_1 \neq 0$ or $U_1 < 0$ or $U_1 > \beta R_d^2(H_1+H_2)/H_1$. Alternatively, we can write the criteria in terms of the vertical shear: $\delta V \neq 0$ or $\delta U > \beta g' H_2/f_0^2$ or

$\delta U < -\beta g' H_1/f_0^2$. As in the shear layer case, this will prove to be the necessary condition for instability.

The perturbation equations for disturbances of the form $\exp(\imath kx + \imath \ell y - \imath \omega t)$ become

$$(kU_n + \ell V_n)q'_n + (k\frac{\partial}{\partial y}Q_n - \ell\frac{\partial}{\partial x}Q_n)\psi'_n = \omega q'_n$$

with

$$\begin{pmatrix} q'_1 \\ q'_2 \end{pmatrix} = \begin{pmatrix} -k^2 - \ell^2 - F_1 & F_1 \\ F_2 & -k^2 - \ell^2 - F_2 \end{pmatrix} \begin{pmatrix} \psi'_1 \\ \psi'_2 \end{pmatrix}$$

and give growth rates as shown in figure 5.xx. In these examples, the shear is fixed in magnitude at $2\beta R_d^2$ (order 10 cm/s) but varied in angle. The case in which the flow is eastward is stable; some wavenumbers will have positive growth rates whenever the PV gradient changes sign in either the x or y direction. The instability conditions above are necessary and sufficient. For example, the standard zonal case has ω/k being the eigenvalue of

$$\begin{pmatrix} \delta U & 0 \\ 0 & 0 \end{pmatrix} + \begin{pmatrix} \beta + F_1\delta U & 0 \\ 0 & \beta - F_2\delta U \end{pmatrix} \begin{pmatrix} -k^2 - F_1 & F_1 \\ F_2 & -k^2 - F_2 \end{pmatrix}^{-1}$$

For $\delta U = \beta/F_2$, the second row of the matrix is zero, and the eigenvalue will be a double root when the upper left element vanishes: when $k = [F_2(F_1 + F_2)]^{1/4}$. For slightly larger δU values, there will be unstable modes in a narrow range of wavenumbers around this value.

Jets and shear layers can exhibit baroclinic instability as well. For example, if we take the flow $U_1 = U\text{sech}^2(y/\ell)$ and $U_2 = 0$, the lower layer PV gradient will be negative at $y = 0$ if $U > \beta/F_2$; the upper layer gradient will be positive everywhere if $\ell > 2/\sqrt{F_1}$ or $U < 24\beta\ell^2/(4-F_1\ell^2)^2$. The instability develops rather differently from the barotropic case, which forms a staggered street of alternating vortices. These can pair and eject dipoles (Flierl, *et al.*, 19xx). In contrast, the baroclinic jet can create rings – sizable volumes of water shifted across the current and detached as the core of a vortex.

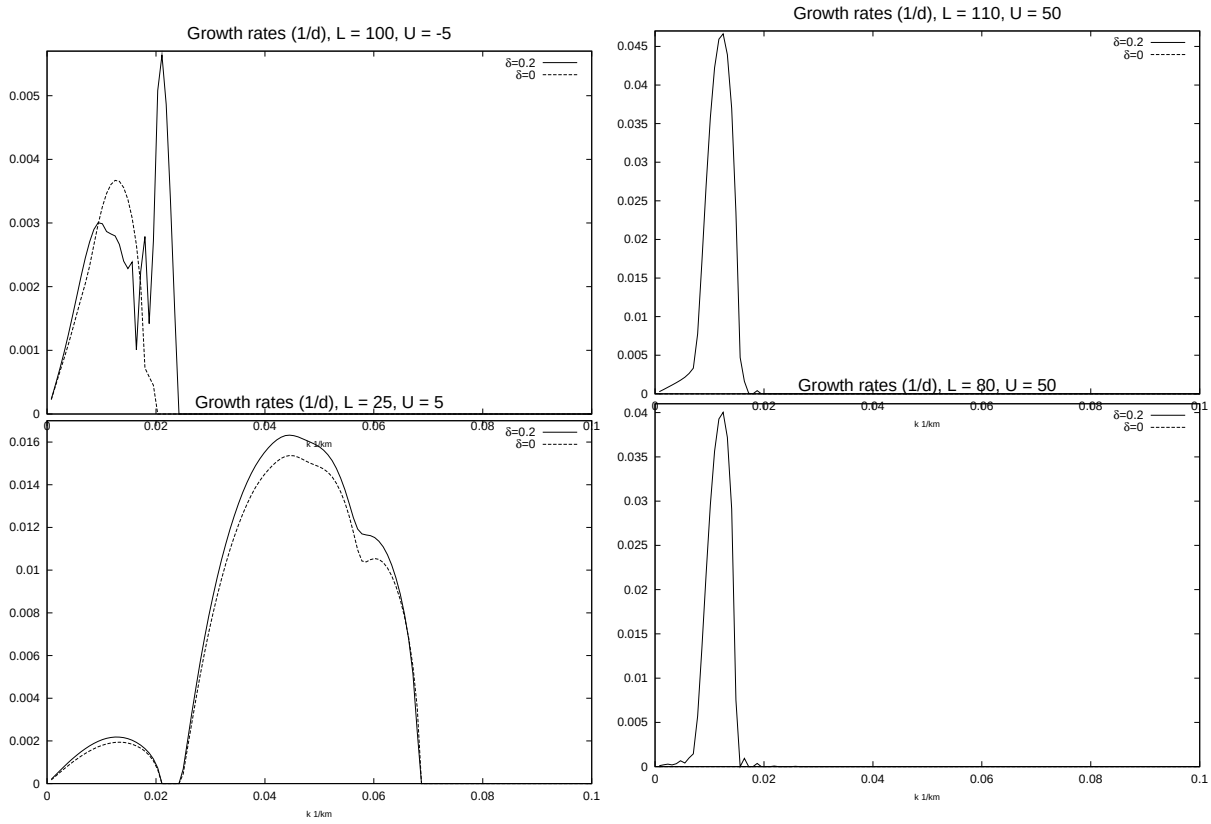

Figure 5.12: Growth rates for the values of ℓ and U_0 listed. The two cases on the right have positive $\frac{\partial}{\partial y}Q_1$ everywhere (and therefore represents a baroclinic instability); in the left two, it changes sign. The dashed lines show the growth rate assuming $H_2 \to \infty$ and indicates instability arising from the horizontal shear.

5.8.5 — Spatial growth

The discussions above (and most studies of instabilities) focus on temporal growth; however, disturbances usually develop in space as well as time. Figure 5.xx illustrates this using a baroclinic jet ($U_0 = 80$, $L = 30$, $R_d = 30$) like the Gulf Stream. The initial disturbance grows, but moves downstream as it does. At any location, the deviation grows for a while and then decays, much like the behavior of a group of waves, except that the peak amplitude gets larger and larger as time or distance downstream increases. Briggs (19xx) develops the theory in detail, while Farrell (19xx) discusses atmospheric applications, and Flierl (19xx) and Ni (19xx) describe the Gulf Stream in more detail and argue that this kind of downstream growth is typical.

The most rapidly growing region moves with the group velocity $c_g = d\Re(\omega)/dk$ evaluated at the wavenumber $k = k_{max}$ where the growth rate curve has a maximum. The envelope magnifies at that peak rate, $max(\sigma) = \Im(\omega(k_{max}))$. This gives a good idea of where the disturbance will be seen. For the example in figure 5.xx, the peak propagates at about 26 km/d and grows with an e-folding time of 5.6 d.

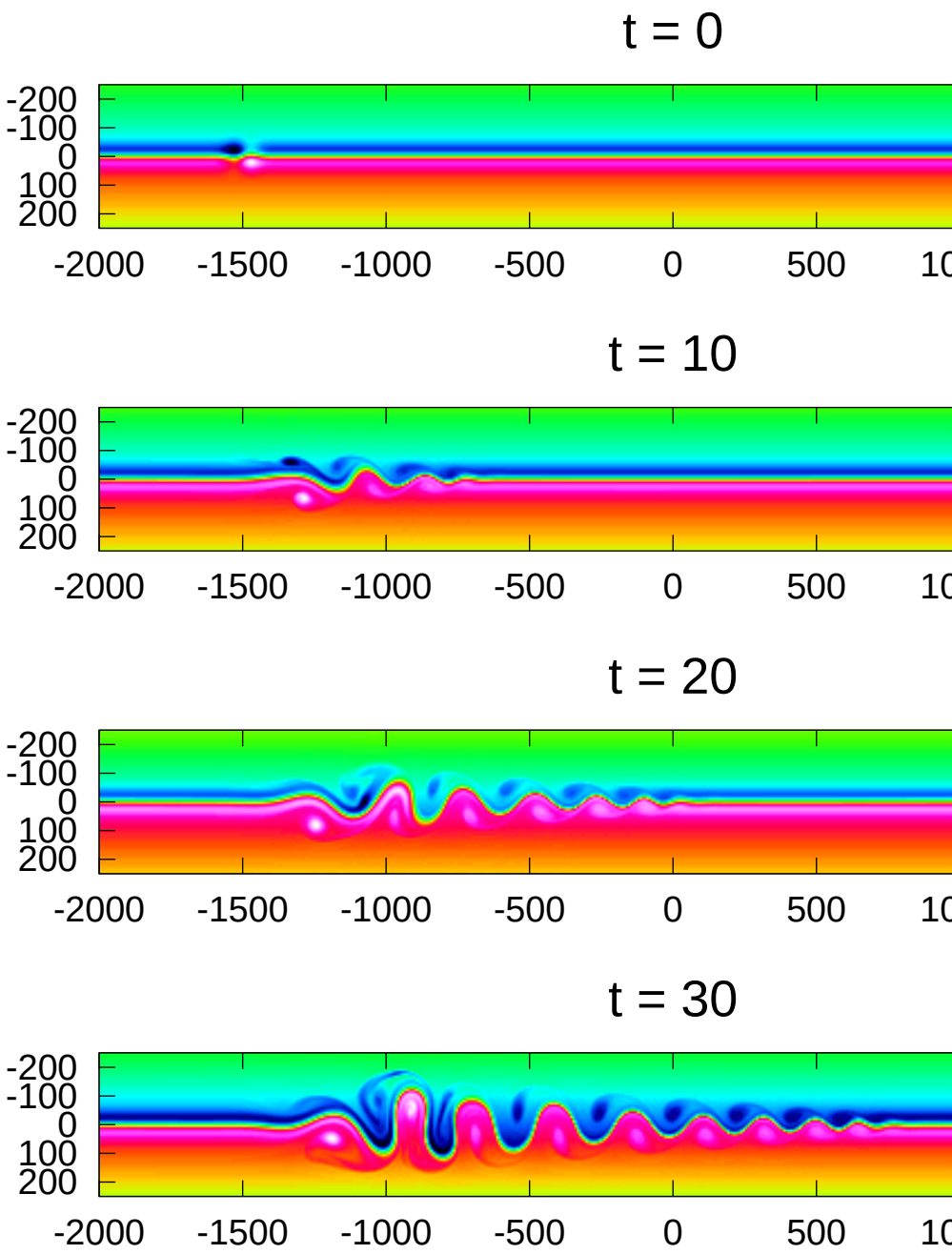

Fig 5.13: Development of a localized disturbance in a baroclinic jet

5.8.6 — Waves

We finish our discussion of instabilities with another rarely discussed topic: the breakdown of regular wave trains. For Rossby waves, Lorenz (19xx) (see also Mied, 18xx, Tung, 19xx, Kim, 19xx) demonstrated that perturbations will grow via a shear instability or, at small amplitude, by interacting with two other waves forming a resonant triad. Roughly speaking, the interaction occur beetween triads of waves satisfying $\mathbf{k}_1 - \mathbf{k}_2 = \mathbf{k}$, so that the nonlinear term between wavenumber k and k_2 projects on k_1 and vice-versa. Although energy flows towards both larger and smaller scales, in most cases a larger fraction goes upscale (Mied, 19xx, Fu and Flierl, 19xx). When the flow velocity is less than the phase speed, the frequencies must also match $\omega_1 - \omega_2 = \omega$, and the transfer favors low-frequency modes with predominantly zonal flows.

5.9 — Surface and bottom boundary layers

Many fluid problems have inhomogeneous dynamics: in some areas particular terms are negligible while in others they become dominant. These differences are usually associated with nearness to a boundary. In the interior of the ocean, friction and diffusion are relatively weak, but these processes become significant in layers near the surface and bottom. Large-scale models include special modules to simulate the distribution and mixing of heat, salt, and momentum, especially in the surface layer. The enhanced mixing also has significant biological impact; for example, it means that phytoplankton will experience a range of light levels over relatively short periods. The processes producing the mixing can be viewed as convective, shear, and Kelvin-Helmholtz instability, but all far above their linear stability thresholds so that the motions are turbulent (e.g., figures 5.xx, 5.xx).

All such models involve parameterizations which attempt to represent the motions on scales which are too small to be resolved by the model grid (often 10's of meters vertically, but much larger horizontally). To understand the issue, let us consider a Reynolds decomposition into an average $\overline{\mathbf{u}}$ and the deviation $\mathbf{u}' = \mathbf{u} - \overline{\mathbf{u}}$. The average is presumed to be a linear operator with the property that $\overline{\overline{g}} = \overline{g}$. Although an ensemble average is perhaps conceptually the cleanest, it does not necessarily yield a scale separation; an alternative method – splitting the spectrum into small and large scales with a top-hat filter – ensures that but may not make sense if the division is not in a spectral gap where the energy is relatively low. The averaged equations

$$\frac{\partial}{\partial t}\overline{\mathbf{u}} + (f\hat{\mathbf{z}} + \overline{\boldsymbol{\zeta}}) \times \overline{\mathbf{u}} + \overline{\boldsymbol{\zeta}' \times \mathbf{u}'} = -\nabla(\overline{\phi} + \frac{1}{2}\overline{\mathbf{u}}^2 + \frac{1}{2}\overline{\mathbf{u}'^2}) + \overline{B}\hat{\mathbf{z}} + \nu\nabla^2\overline{\mathbf{u}}$$

$$\nabla \cdot \overline{\mathbf{u}} = 0$$

$$\frac{\partial}{\partial t}\overline{B} + \nabla \cdot (\overline{\mathbf{u}}\overline{B}) + \nabla \cdot (\overline{\mathbf{u}'B'}) = \kappa\nabla^2\overline{B}$$

$$\frac{\partial}{\partial t}\overline{b}_i + \nabla \cdot (\overline{\mathbf{u}}\,\overline{b}_i) + \nabla \cdot \overline{\mathbf{u}'b_i'} = \overline{\mathcal{B}_i(\overline{\mathbf{b}} + \mathbf{b}')} + \kappa_b\nabla^2\overline{b}_i$$

show that we need information about the eddy terms such as the buoyancy flux $\overline{\mathbf{u}'B'}$ in order to predict change in $\overline{\mathbf{u}}$, $\overline{B}$, or $\overline{b}$. Parameterizations attempt to represent the eddy fluxes in terms of the average fields, e.g. $\overline{\mathbf{u}'b_i'} \simeq -\kappa_{eddy}\nabla\overline{b}_i$. Flierl and McGillicuddy (19xx)

explore the applicability of this approximation and argue that it may not be appropriate; we shall discuss this further in chapter xx. Other models use the resolved, larger-scale fields to decide which layers mix with which. The mixing may well be nonlocal in the sense that the flux across a face of a volume depends on the whole structure of the flow and density fields. For example, consider convective adjustment in a region with a negative graient of buoyancy at the surface and a positive one below. If the successive values going upwards are $-1/2, -1/4, 0, -1$, then the adjustment will begin by mixing the top two layers giving $-1/2, -1/4, -1.2, -1/2$; then the top three boxes will be mixed so that fluid having a positive gradient initially is nevertheless strongly mixed (giving a final profile of $-1/2, -5/12, -5/12, -5/12$).

For a full review of surface layer models, see xxx (19xx); choice of approach may be governed by the scheme selected when the physical model was built, or by the degree of abstraction desired. Here, we discuss several eaxamples rather briefly to give an idea of the physics included; in examining the seasonal cycle (chapter xx), we shall see that the biological responses temd to be pretty similar.

CA

Dewar (19xx) studied a number of models to look at the behavior under various conditions and concluded that properties like the mixed layer depth (MLD) and surface buoyancy could be reproduced by a simple system assuming either convective adjustment (under cooling) or instantaneous mixing to a fixed depth, because of wind-driven turbulence (under heating). Figure xx shows a seasonal cycle (after a 4 year spin-up). Including the diurnal cycle makes a big difference when the heating is considered as a surface forcing or when the wind-mixed MLD is set to zero, but alters these experiments (which have separate decay scales for the 62% of the energy in the red and the 38% in the blue parts of the spectrum: 0.6 and 20 m respectively) very little.

Ri

Convective adjustment in effect postulates an infinite mixing coefficient whenever the local gradient in buoyancy, determined by the differences between cells, becomes negative. Making κ a function of the gradient, having a large, but finite, value when $\frac{\partial}{\partial z}B < 0$ gives very similar results except the heating is trapped in the surface layer in the summer, much like the case with no wind-driven MLD above. This shallow thermocline is eroded by the wind-driven shears gnerating Kelvin-Helmholtz instability. Thus, if we add wind and take

$$\kappa_{eddy}(Ri) = \kappa_{min} + \kappa_{max}(Ri < \frac{1}{4})$$

(e.g., Philander and Pacanowski,19xx,), this feature disappears and the temperature profiles become very similar to the other models. Note that the large range of viscosities can be handled easily using an implicit scheme. This is an example of a local model.

PWP

The Price-Weller-Pinckel model combines a number of these ideas to see how well the resulting model can compare with observations. They apply the thermal forcing (or, more generally, buoyancy forcing including evaporation and percipitation) and convectively adjust the density and velocities. The wind stress is applied over the MLD as set by the convection ($\tau/\rho_0 h_{ml}$).

Further mixing takes place until the "bulk Richardson number $\Delta B h_{ml}/|\Delta \mathbf{u}|^2$ is smaller than one. The Δ's are the differences across the mixed layer base; this idea from Pollard *et al.*(19xx) does not have a grounding in stability theory, but made sense dimensionally when the detailed vertical structure is not resolved and the only property the parameterization needs to predict is the MLD. In the PWP model, this step seems less necessary, since the local Ri will be small so that the mixing described next will occur.

The last step is mixing based on the local Richardson number $Ri = \Delta B dz/|\delta \mathbf{u}|^2$ with dz the grid spacing. If the smallest value of this is less than 1/4, then the associated pair of boxes is mixed back towards neutrality. This may make the Richardson number at the next interface up or down subcritical, so the test and mixing is iterated until Ri is everywhere greater than the critical value. Because this stage can require multiple passes (peaking at 10000 in one time step of the seasonal example), it can be quite inefficient when multiple biological variables are considered.

k-epsilon and MY

Parameterization is a form of the closure problem: to predict the mean, we need second moments, to predict the second moments (like $\overline{\mathbf{u}'B'}$), we need third moments, etc. The Richardson number based closures are first order in that fluxes are functionals of the mean variables. The higher order closure turbulence models, on the oter hand, base their eddy viscosities on properties of the unresolved turbulence such as the eddy kinetic energy $K = \frac{1}{2}\overline{|\mathbf{u}'|^2}$ and the turbulent dissipation rate $\mathcal{E} = \nu\overline{(\nabla_j u_i')^2}$. From the biological point of view, the physical model is predicting the mixing rates

$$\kappa_{eddy} = \frac{K^2}{\mathcal{E}} S_B(Ri')$$

The eddy Richardson number $Ri' = \frac{\partial B}{\partial z} K^2/\mathcal{E}^2$ corrects the nondimensional function S_B for stratification effects (e.g., Galperin *et al.*, 1988). Dimensional analysis dictates the form of the coefficient (and relates it to the mixing length theory of Prandtl, 19xx); as mentioned in chapter 1 and discussed in more detail in chapter xx, we cannot generally expect the fluxes to depend only on the local gradient of a field. Indeed, in the convection experiment above, $\overline{w'B'}$ is related to the penetrative radiation, not the local buoyancy gradient; on the other hand, using a greatly enhanced diffusivity in the regions where $Ri < 0.25$ produces reasonable buoyancy profiles.

For a rough understanding of the physics, in these models, let us examine the eddy kinetic energy equation

$$\frac{\partial}{\partial t} K + \overline{\mathbf{u}} \cdot \nabla K = -\overline{u_i' u_j'} \nabla_j \overline{u}_j + \overline{w'B'} - \mathcal{E} - \nabla \cdot \overline{\mathbf{u}'\phi'} - \nabla_j \frac{1}{2} \overline{u_j' u_i'^2} + \nabla \nu \nabla K$$

Using the eddy viscosities gives

$$\frac{\partial}{\partial t}K + \overline{\mathbf{u}} \cdot \nabla K = \nu_{eddy}\left[\frac{1}{2}\frac{\partial \overline{u}_i}{\partial x_j} + \frac{1}{2}\frac{\partial \overline{u}_j}{\partial x_i}\right]^2 - \kappa_{eddy}\frac{\partial \overline{B}}{\partial z} - \mathcal{E} - \nabla \cdot \overline{\mathbf{u}'\phi'} - \nabla_j \frac{1}{2}\overline{u_j' u_i'^2} + \nabla\nu\nabla K$$

and the closure assumption replaces the unknown higher order terms with an eddy diffusion of K

$$\frac{\partial}{\partial t}K + \overline{\mathbf{u}} \cdot \nabla K = \nu_{eddy}\left[\frac{1}{2}\frac{\partial \overline{u}_i}{\partial x_j} + \frac{1}{2}\frac{\partial \overline{u}_j}{\partial x_i}\right]^2 - \kappa_{eddy}\frac{\partial \overline{B}}{\partial z} - \mathcal{E} + \nabla(\nu + \nu_{eddy})\nabla K$$

A similar equation for the dissipation

$$\frac{\partial}{\partial t}\mathcal{E} + \overline{\mathbf{u}} \cdot \nabla \mathcal{E} = \frac{\mathcal{E}}{K}\left[C_1\nu_{eddy}\left(\frac{1}{2}\frac{\partial \overline{u}_i}{\partial x_j} + \frac{1}{2}\frac{\partial \overline{u}_j}{\partial x_i}\right)^2 - C_2\mathcal{E} - C_3\kappa_{eddy}\frac{\partial \overline{B}}{\partial z}\right] + \nabla(\nu + \nu_{eddy})\nabla\mathcal{E}$$

presumes that the dissipation is relaxing back to some fraction of the production with the turbulent time scale $K/\mathcal{E}$. These equations then produce eddy coefficients which vary in space and time as the flow evolves.

The "level 2.5" scheme produced by Mellor and Yamada is quite similar to the k-ϵ model, although it's posed in terms of K and an eddy length scale ($\sim K^{3/2}/\mathcal{E}$) instead. However, they have also produced more complex (and therefore rarely used) approaches which track the time and space evolution of the Reynolds stresses themselves.

KPP

Finally, we describe the "K profile parameterization" model (Large, *et al.*, 1994) which has become popular. Like PWP, it synthesizes a number of previous approaches. The eddy fluxes are computed diagnostically (without requiring additional dynamic fields) but now have both a local component, still represented using an eddy viscosity/ diffusivity, and a nonlocal part representing the effects of the largest scale turbulent eddies. However, the non-local transports act only on temperature and salinity and only when the surface fluxes are destabilizing. For scalars with no fluxes at the surface, the diffusivity is a product of the mixed layer depth h_{ml}, a velocity scale $w_s(-z/h_{ml})$, and a nondimensional shape function $G(-z/h_{ml})$ which is a cubic polynomial. The coefficients are chosen to force the eddy diffusivity to be zero at the surface and to match to the very small interior value at the base of the mixed layer. The velocity scale varies with z/h_{MO} where h_{MO} is the Monin-Obukov length $|\tau/\rho|^{3/2}/0.4Q(0)$, a measure of the scale over which wind-driven eddies can overcome a stable density gradient. In the deeper water, the velocity scale is uniform.

For the biological fields, the mixing remains local; however, the KPP scheme differs from $\kappa(Ri)$ in that it combines information from various regions.

5.10 — Appendix A

5.10.1 — Cartesian

Gradient:

$$\nabla\phi = (grad\ \phi) = \begin{pmatrix} \frac{\partial}{\partial x}\phi \\ \frac{\partial}{\partial y}\phi \\ \frac{\partial}{\partial z}\phi \end{pmatrix}$$

Divergence:

$$\nabla \cdot \mathbf{F} = div\ \mathbf{F} = \frac{\partial}{\partial x}F_x + \frac{\partial}{\partial y}F_y + \frac{\partial}{\partial z}F_z$$

Curl:

$$\nabla \times \mathbf{F} = curl\ \mathbf{F} = \begin{pmatrix} \frac{\partial}{\partial y}F_z - \frac{\partial}{\partial z}F_y \\ ;\frac{\partial}{\partial z}F_x - \frac{\partial}{\partial x}F_z \\ \frac{\partial}{\partial x}F_y - \frac{\partial}{\partial y}F_x \end{pmatrix}$$

5.10.2 — Polar (lab)

The coordinates are r, θ and z, realted to the Cartesian forms by

$$\begin{aligned} x &= r\cos\theta \\ y &= r\sin\theta \\ z &= z \end{aligned}$$

The operators become:
Gradient:

$$;\nabla\phi = (grad\ \phi) = \begin{pmatrix} \frac{\partial}{\partial r}\phi \\ \frac{1}{r}\frac{\partial}{\partial\theta}\phi \\ \frac{\partial}{\partial z}\phi \end{pmatrix}$$

Divergence:

$$\nabla \cdot \mathbf{F} = div\ \mathbf{F} = \frac{1}{r}\frac{\partial}{\partial r}[rF_r] + \frac{1}{r}\frac{\partial}{\partial\theta}F_\theta + \frac{\partial}{\partial z}F_z$$

Curl:

$$\nabla \times \mathbf{F} = curl\ \mathbf{F} = \begin{pmatrix} \frac{1}{r}\frac{\partial}{\partial\theta}F_z - \frac{\partial}{\partial z}F_\theta \\ \frac{\partial}{\partial z}F_r - \frac{\partial}{\partial r}F_z \\ \frac{1}{r}\frac{\partial}{\partial r}[rF_\theta] - \frac{1}{r}\frac{\partial}{\partial\theta}F_r \end{pmatrix};$$

5.10.3 — Earth coords.

We consider the case of earth coordinates: longitude (λ), latitude (θ) , and height (z). We can define these by

$$\begin{aligned} x &= (a+z)\cos\theta\sin\lambda \\ ;\ y &= (a+z)\cos\theta\cos\lambda \\ z &= (a+z)\sin\theta \end{aligned}$$

where a is the radius of the planet. (One could work with ellipsoids to represent the flattened shape, but it is rarely worth the effort.) The operators are given below.
Gradient:

$$\nabla\phi = (grad\ \phi) = \begin{pmatrix} \frac{1}{(a+z)\cos\theta}\frac{\partial}{\partial\lambda}\phi \\ \frac{1}{(a+z)}\frac{\partial}{\partial\theta}\phi \\ \frac{\partial}{\partial z}\phi \end{pmatrix}$$

Divergence:

$$\nabla\cdot\mathbf{F} = div\ \mathbf{F} = \frac{1}{(a+z)\cos\theta}\frac{\partial}{\partial\lambda}F_\lambda + \frac{1}{(a+z)\cos\theta}\frac{\partial}{\partial\theta}(\cos\theta F_\theta) + \frac{1}{(a+z)^2}\frac{\partial}{\partial z}([a+z]^2F_z)$$

Curl:

$$\nabla \times \mathbf{F} = curl\ \mathbf{F} = \begin{pmatrix} \frac{1}{(a+z)}\frac{\partial}{\partial\theta}F_z - \frac{1}{(a+z)}\frac{\partial}{\partial z}[(a+z)F_\theta] \\ \frac{1}{(a+z)}\frac{\partial}{\partial z}[(a+z)F_\lambda] - \frac{1}{(a+z)\cos\theta}\frac{\partial}{\partial\lambda}F_z \\ \frac{1}{(a+z)\cos\theta}\frac{\partial}{\partial\lambda}F_\theta - \frac{1}{(a+z)\cos\theta}\frac{\partial}{\partial\theta}[\cos\theta F_\lambda] \end{pmatrix}$$

Usually the $(a+z)$ terms are replaced by a.

5.11 — Appendix : Numerical methods

For example, suppose we solve

$$\frac{\partial}{\partial t}S = -U\frac{\partial}{\partial x}S$$

; by a simple forward step and upwind difference

$$S(x, t+\delta t) = S(x,t)\left(1 - \frac{U\delta t}{\delta x}\right) + \frac{U\delta t}{\delta x}S(x-\delta x, t)$$

If we consider an initial condition which has a single non-zero value, $S(0,0) = 1$ the point to the right will have a larger value at δt if $U > \delta x/\delta t$ and the original point will become negative. Both of these situations are inconsistent with the continuum equation. Continuing, we'd find

$$; S(n\delta x, n\delta t) = \left(\frac{U\delta t}{\delta x}\right)^n$$

implying exponential increase in the maximum va;lue when the CFL condition is violated. Indeed, the condition is somewhat more stringent: If we consider an intitial condition of the shortest resolved wave

$$S(n\delta x, 0) = (-1)^n$$

then we find

$$S(n\delta x, t) = A(t)(-1)^{-}n$$

with

$$A(t) = A(0)\left(1 - 2\frac{U\delta t}{\delta x}\right)^{t/\delta t}$$

Thus, if $U\delta t/\delta x < 0.5$ the wave will damp out; if $U\delta t/dx > 0.5$ it will grow exponentially. Since the equation can be viewed as either an advection equation or a one-d wave equation, we conclude that the time step will be limited by the fastest speeds.